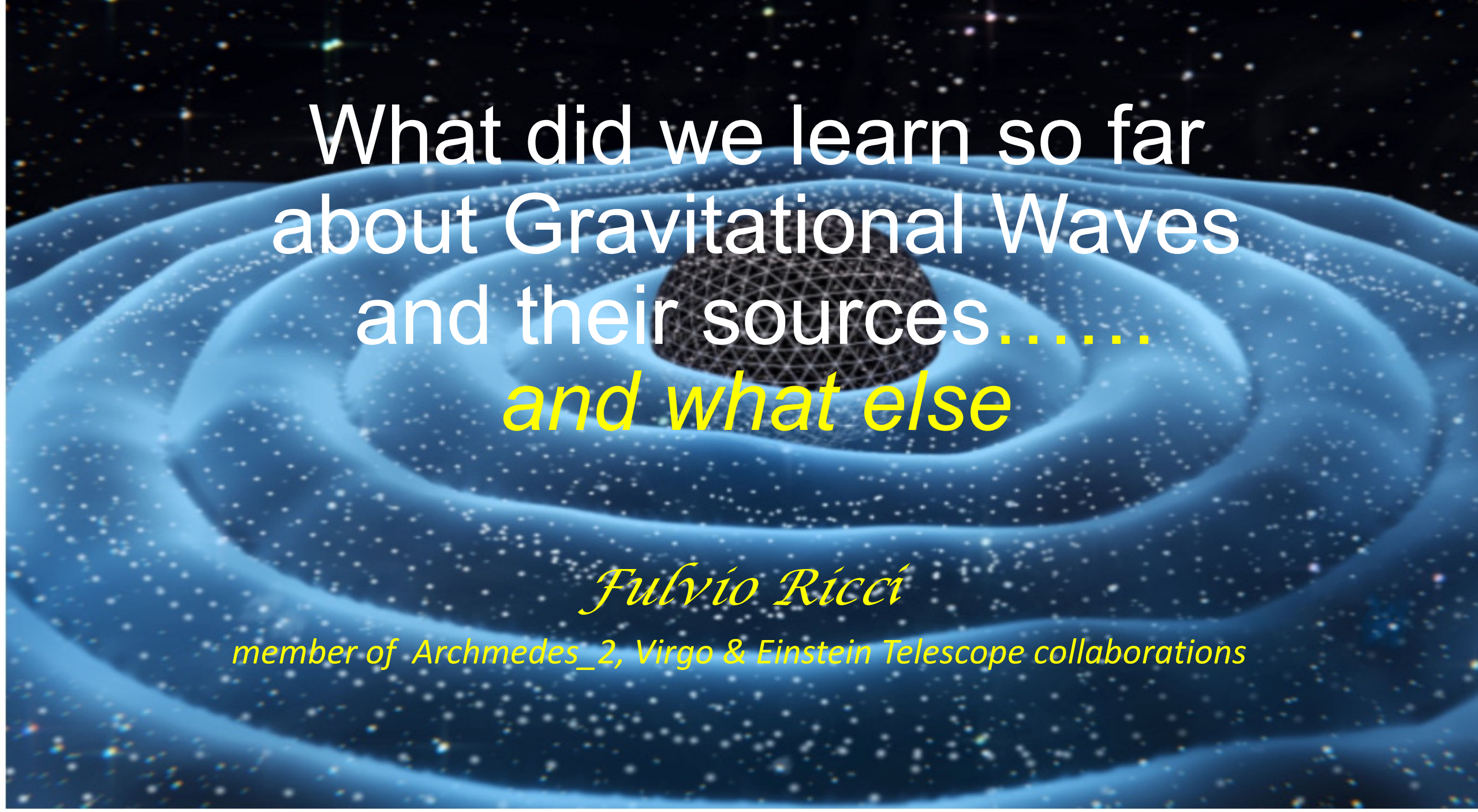

Fulvio Ricci

member of Archmedes_2, Virgo & Einstein Telescope collaborations

Talk Outline

- Introduction to Gravitational Waves (GW) and the detectors
- GW discoveries
- A glance to the future of GW
- Conclusions

Introduction to GW and the detectors

General Relativity and GW in a single slide

Space time rigidity constant 1/N

$K = 8\pi G/c^4 \sim 10^{-44}$ 1/N

Huge energy nedeed to strain the space time: low wave amplitude

Space Time Curvature $1/m^2$

$$G_{\mu\nu} = k\, T_{\mu\nu}$$

Stress energy tensor N/m^2

linearising the equation

$g_{\mu\nu} \sim \eta_{\mu\nu} + h_{\mu\nu}$ with $|h_{\mu\nu}| << 1$

$\eta_{\mu\nu}$ metric tensor of the Minkowski space-time

choosing the TT gauge in the vacuum space

$$\Box h_{\mu\nu} = 0$$

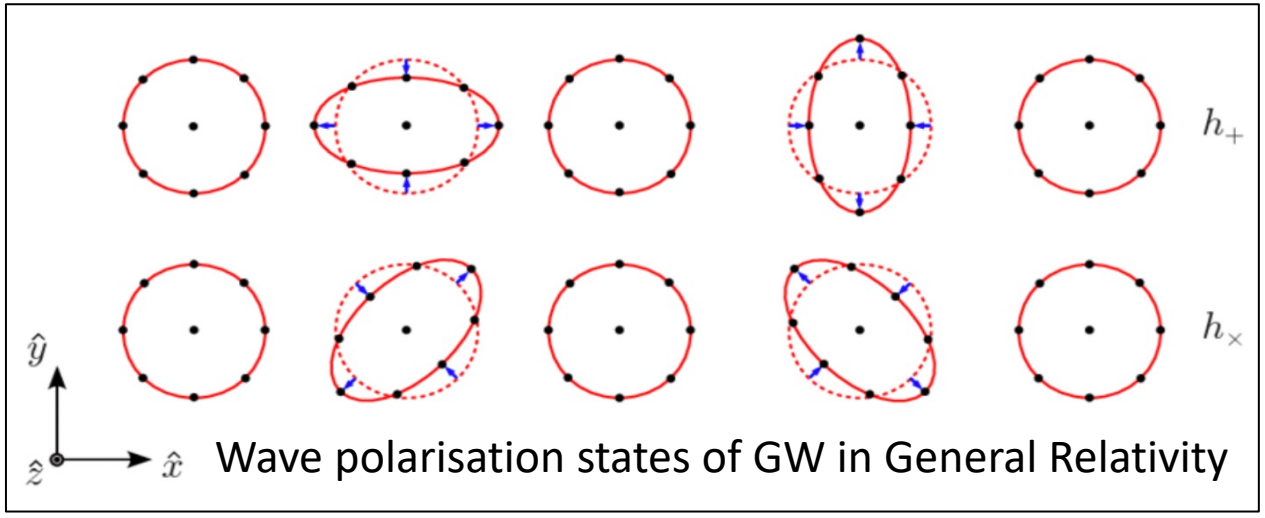

Wave polarisation states of GW in General Relativity

First contribution to radiation emission due to the time change of the quadrupole moment of the source D_{ij}

Luminosity of the GW source

$$L_{GW} = \frac{G}{5c^5} \sum_{ij} \left[\frac{d^3}{dt^3} D_{ij} \right]^2$$

5.5×10^{-54} $m^{-2}\, kg^{-1}\, s^3$

The huge depression factor is compensated by considering as sources compact astrophysical objects moving at high velocity

Detection principle of a GW

The simplest way to probe the metric is to monitor the photon propagation travelling between two free falling test masses in the perturbed space-time metric.

We assume a plane wave with + polarisation h_+ and propagation along z

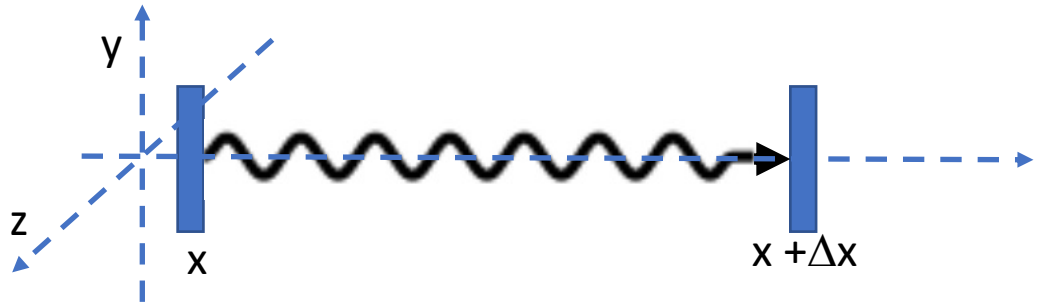

$$h_{xx} = h \sin(kz - \omega t)$$

$0 = \Delta s^2 = c^2 \Delta t^2 - [1 + h \sin(kz - \omega t)] \Delta x^2$ with $\Delta t << 1/\omega$ and $h << 1$ ➔ $c \Delta t \simeq [1 + (h/2)\sin(kz - \omega t)] \Delta x$

$$\frac{\delta(c\Delta t)}{\Delta x} = \frac{h}{2} \sin(kz - \omega t)$$

Strain changing wih time

$$\frac{\delta l}{l} = \frac{h}{2}$$

Measured quantity

GW spectrum

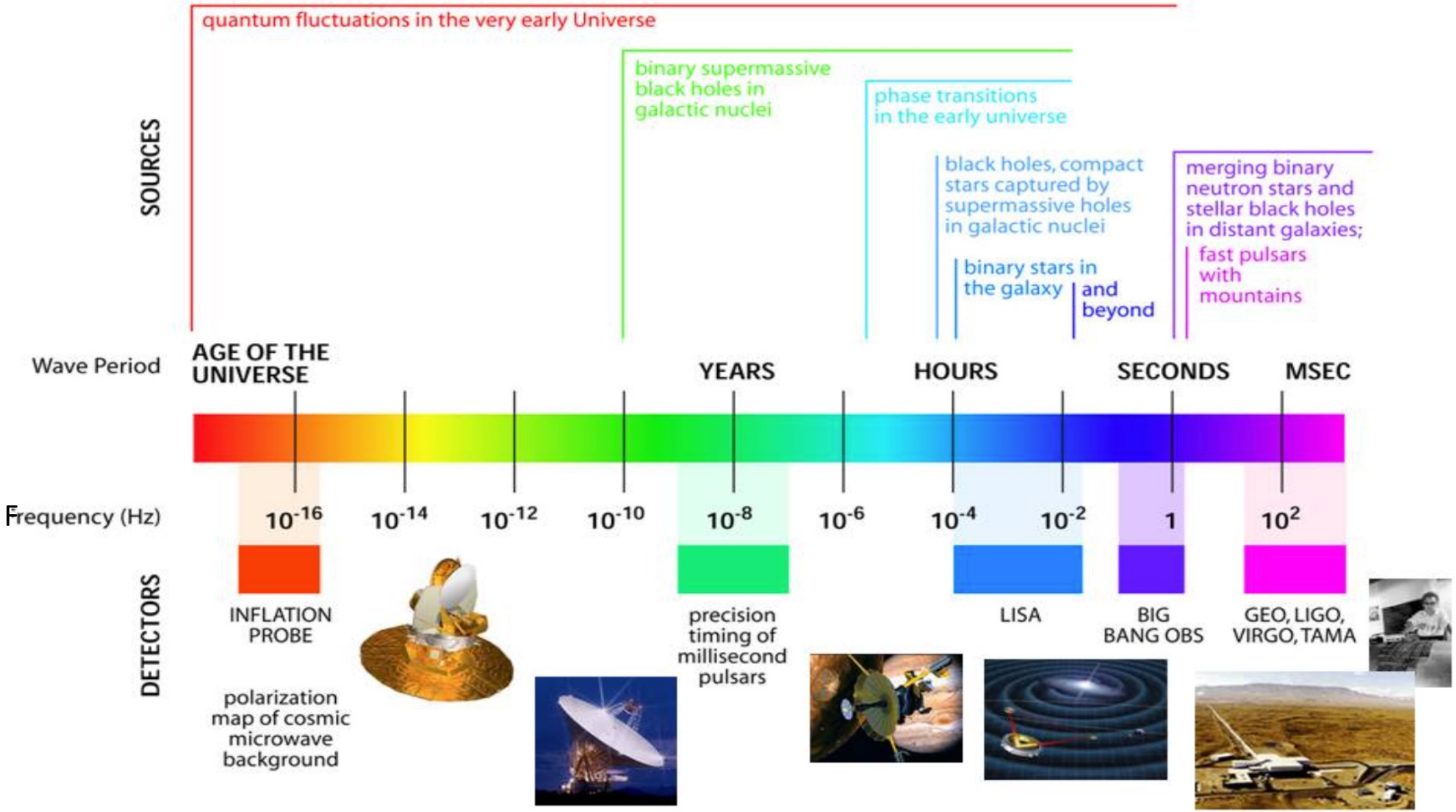
SOURCES
quantum fluctuations in the very early Universe
binary supermassive black holes in galactic nuclei
phase transitions in the early universe
black holes, compact stars captured by supermassive holes in galactic nuclei
merging binary neutron stars and stellar black holes in distant galaxies;
binary stars in the galaxy
and beyond
fast pulsars with mountains
Wave Period
AGE OF THE UNIVERSE
YEARS
HOURS
SECONDS
MSEC
Frequency (Hz)
10^{-16}
10^{-14}
10^{-12}
10^{-10}
10^{-8}
10^{-6}
10^{-4}
10^{-2}
1
10^{2}
DETECTORS
INFLATION PROBE
polarization map of cosmic microwave background
precision timing of millisecond pulsars
LISA
BIG BANG OBS
GEO, LIGO, VIRGO, TAMA

Light and Mirror Motion

The output electric fields are phase modulated by the mirror motion

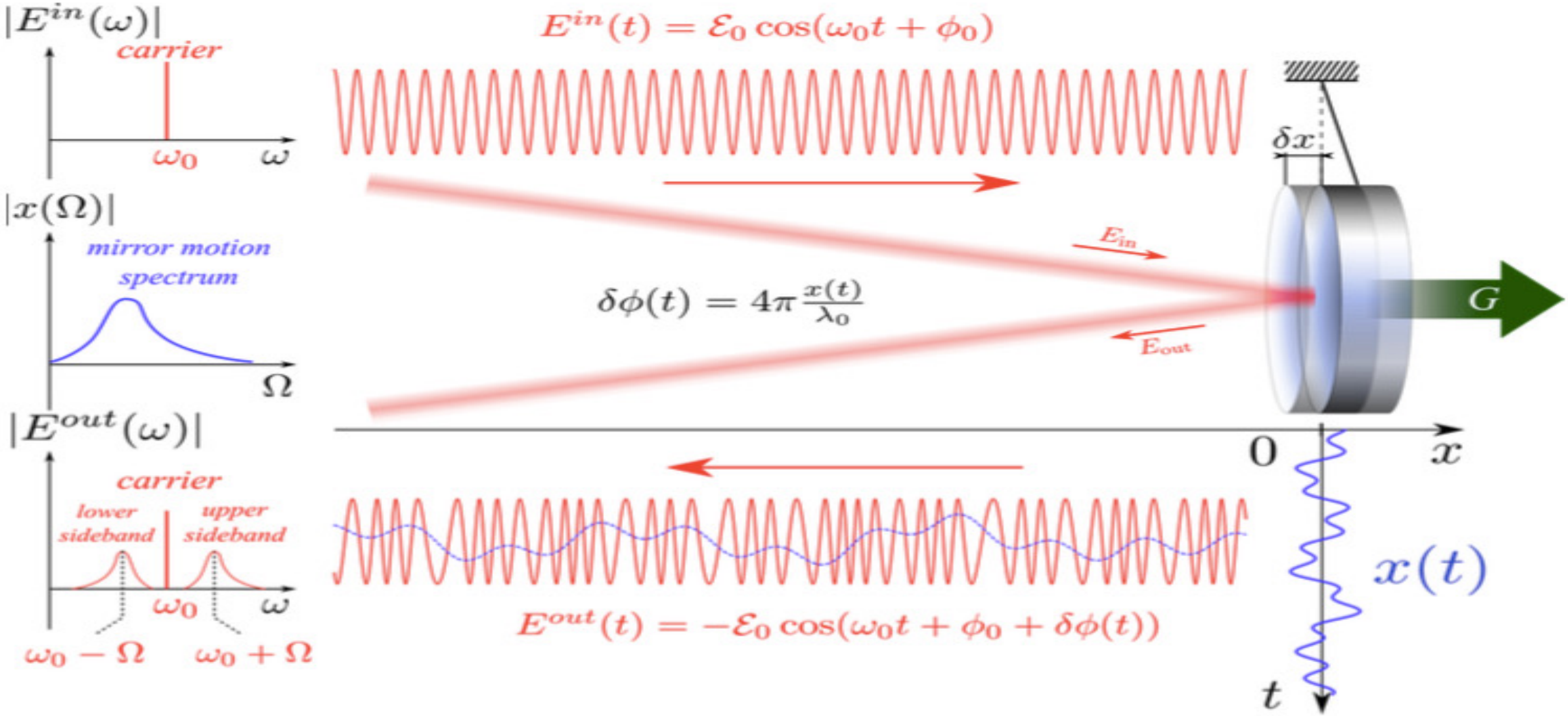

Detectors on the Earth: the interferometers

Quantity to be measured

$\Delta l_{GW} = h\, l$

if $l \sim 1$ km ➔ $\Delta l_{GW} \sim 10^{-18}$ m

$\lambda \sim 10^{-6}$ m *wavelenght of an infrared laser*

$\Delta l \sim 10^{-6} - 10^{-8}$ m *micro-seimic displacements of the Earth ground around 1 Hz*

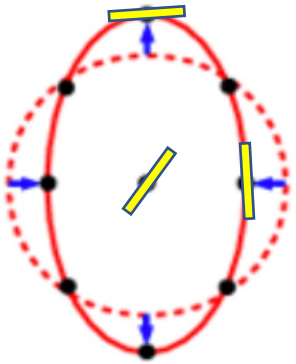

Electric field components in a Michelson Interferometer

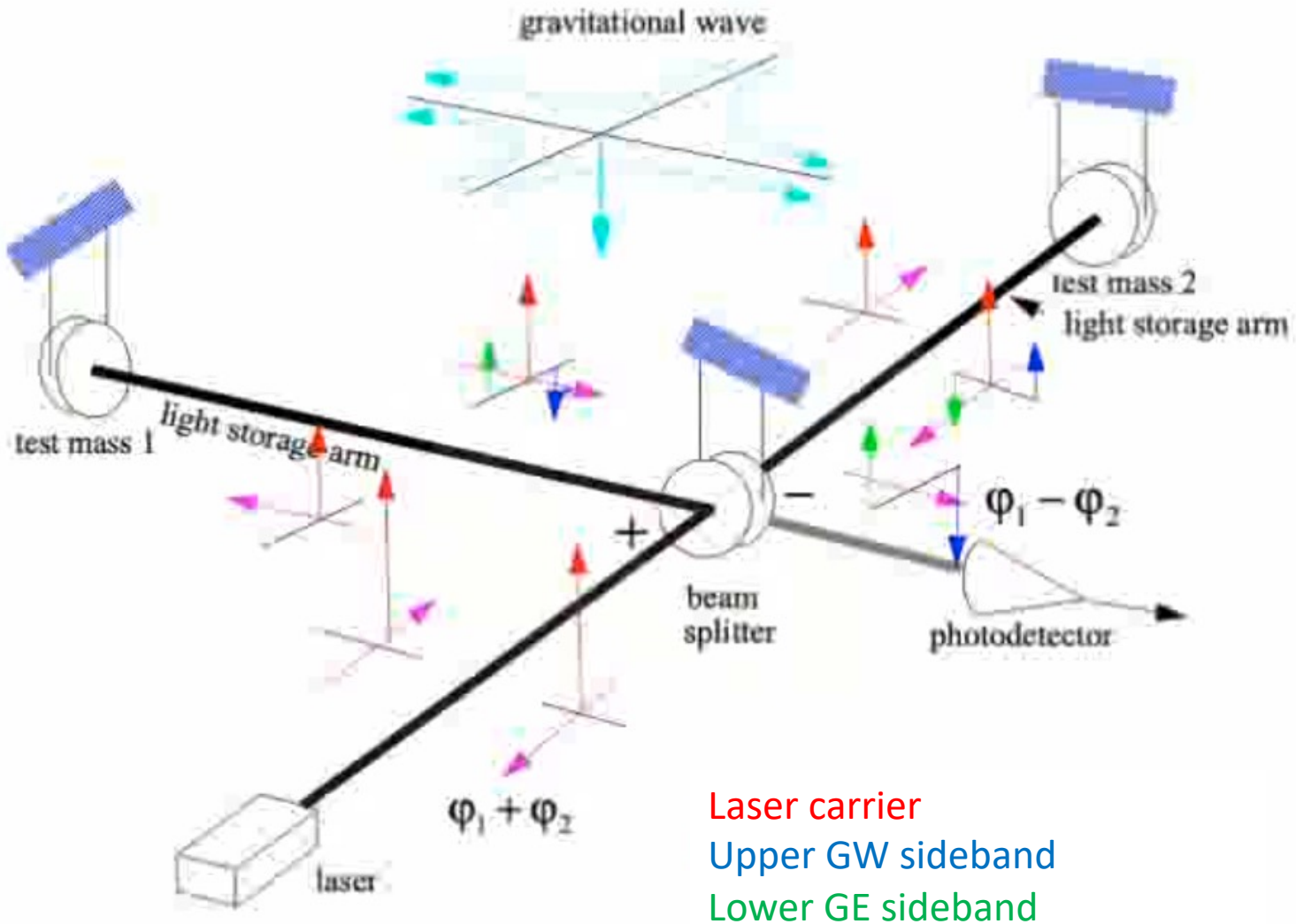

Laser carrier
Upper GW sideband
Lower GE sideband
Propagation idrcion of the light

Credit: R. Weiss

The real detector

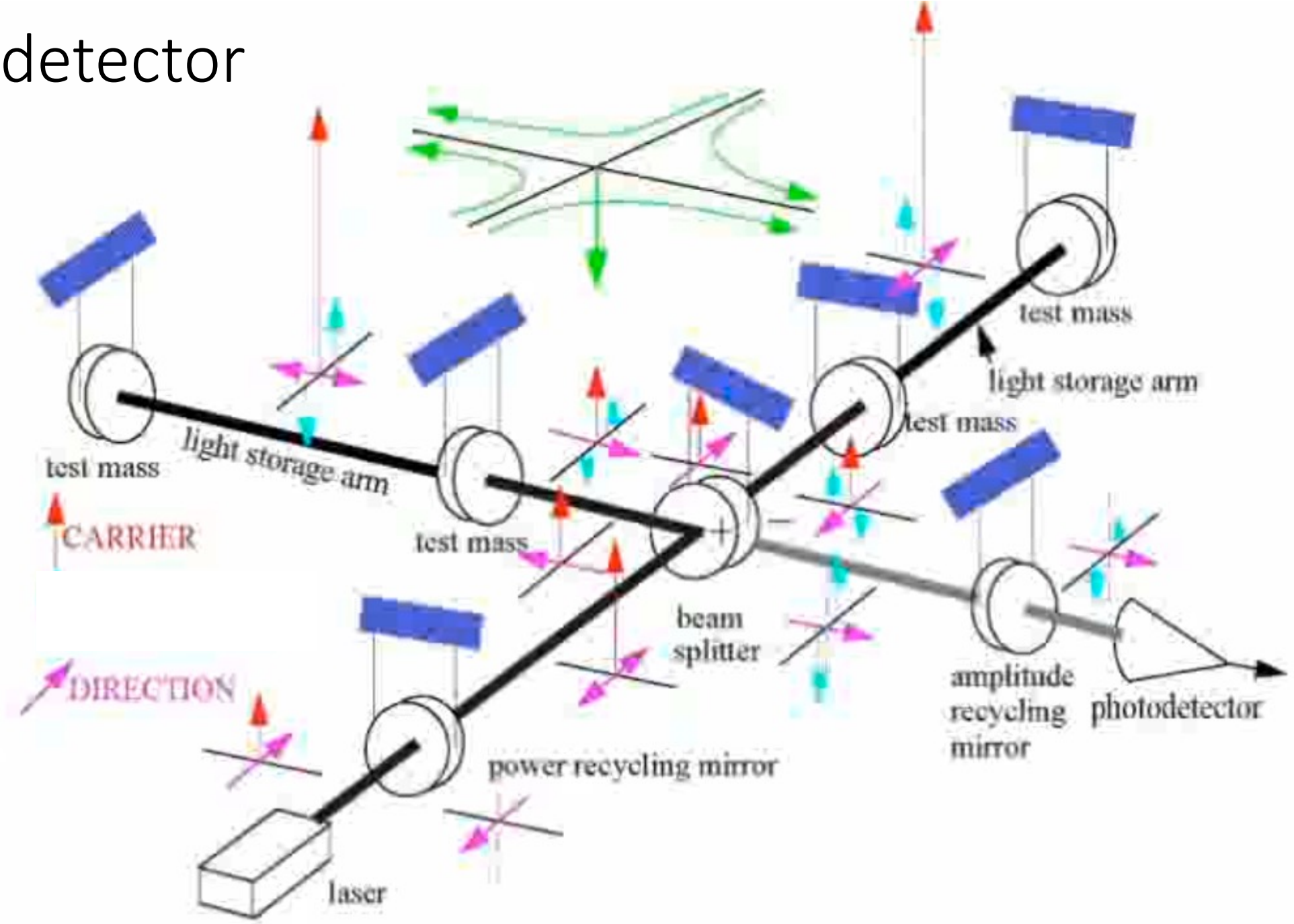

Credits: R. Weiss

Beating Quantum Noise

V.B. Braginsky and F.Y. Khalili: Rev. Mod. Phys. 68 (1996)

While shot noise contribution decreases with optical power, radiation pressure level increases:

$$h_{\rm sn}(f) = \frac{1}{L}\sqrt{\frac{\hbar c\lambda}{2\pi P}}$$

wavelength, optical power, Arm length

$$h_{\rm rp}(f) = \frac{1}{mf^2L}\sqrt{\frac{\hbar P}{2\pi^3 c\lambda}}$$

Mirror mass

- The SQL is the minimal sum of shot noise and radiation pressure noise
- Using a classical quantum measurement the SQL is the lowest achievable noise

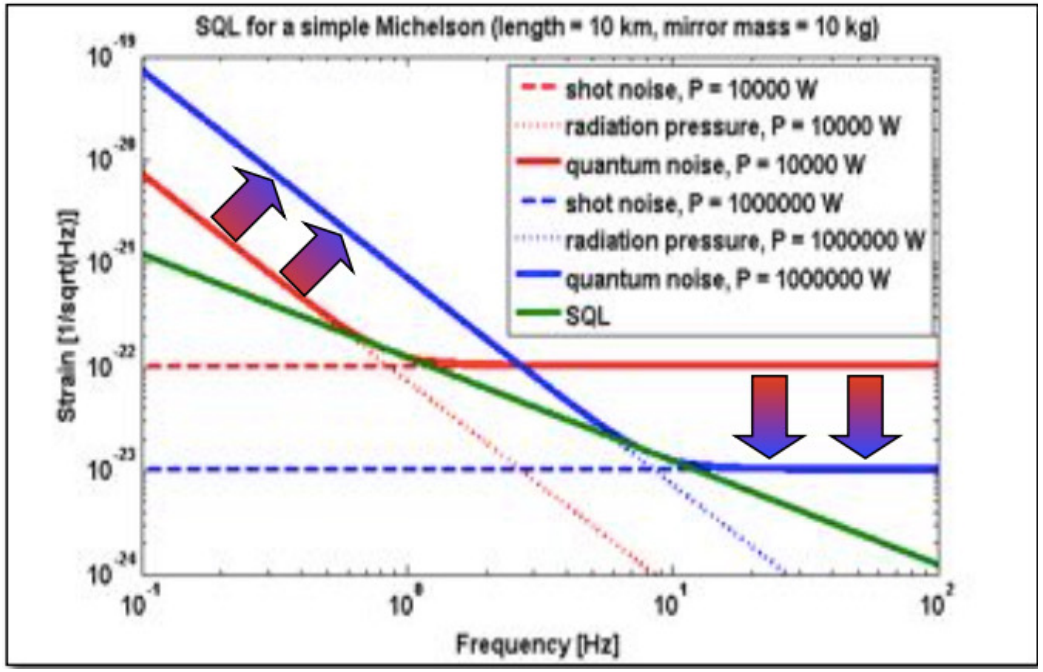

3 dB Squeezed Light Injection, LIGO Livingston, Feb 2019

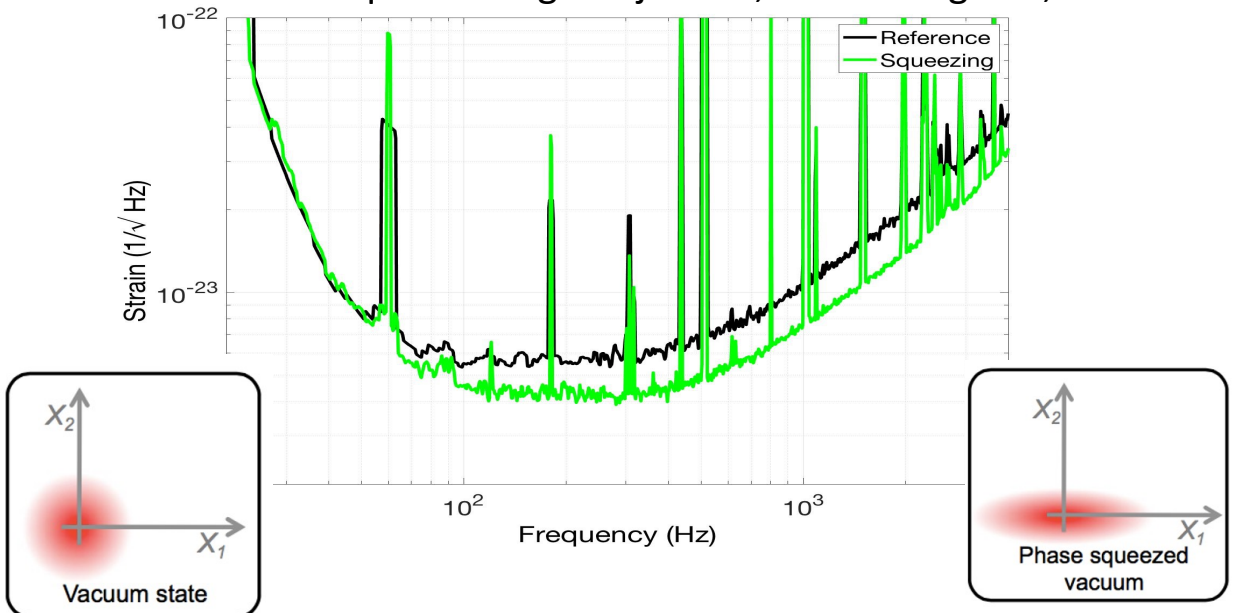

Next run O4. Main Improvement: higher laser power and frequency dependent squeezing

The driving idea

To simultaneously reduce shot noise at high frequencies and quantum radiation pressure noise at low frequencies requires a quantum noise filter cavity with low optical losses to rotate the squeezed quadrature as a function of frequency.

Adopted Method

- Reflect frequency independent squeezing off a detuned Fabry-Perot cavity
- Rotation frequency depends on the cavity line-width

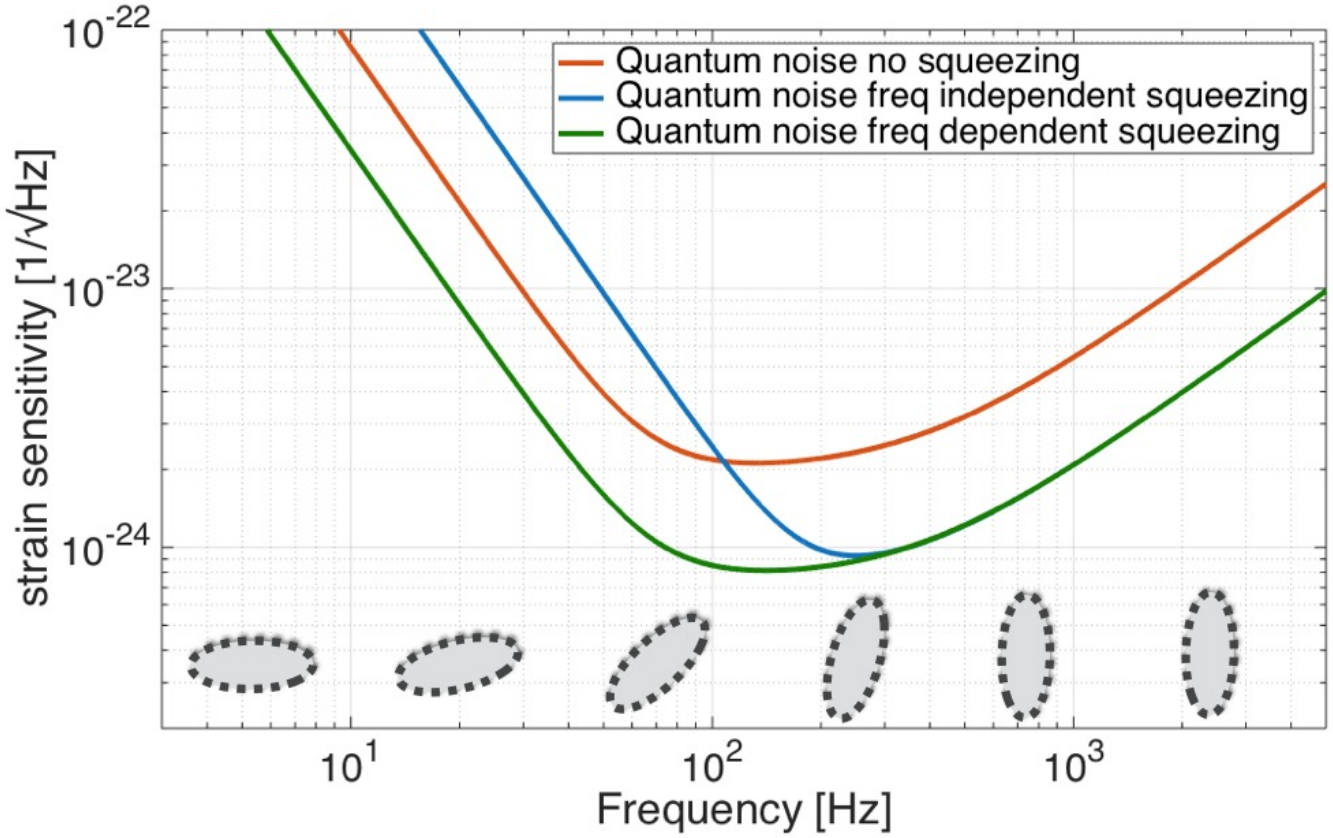

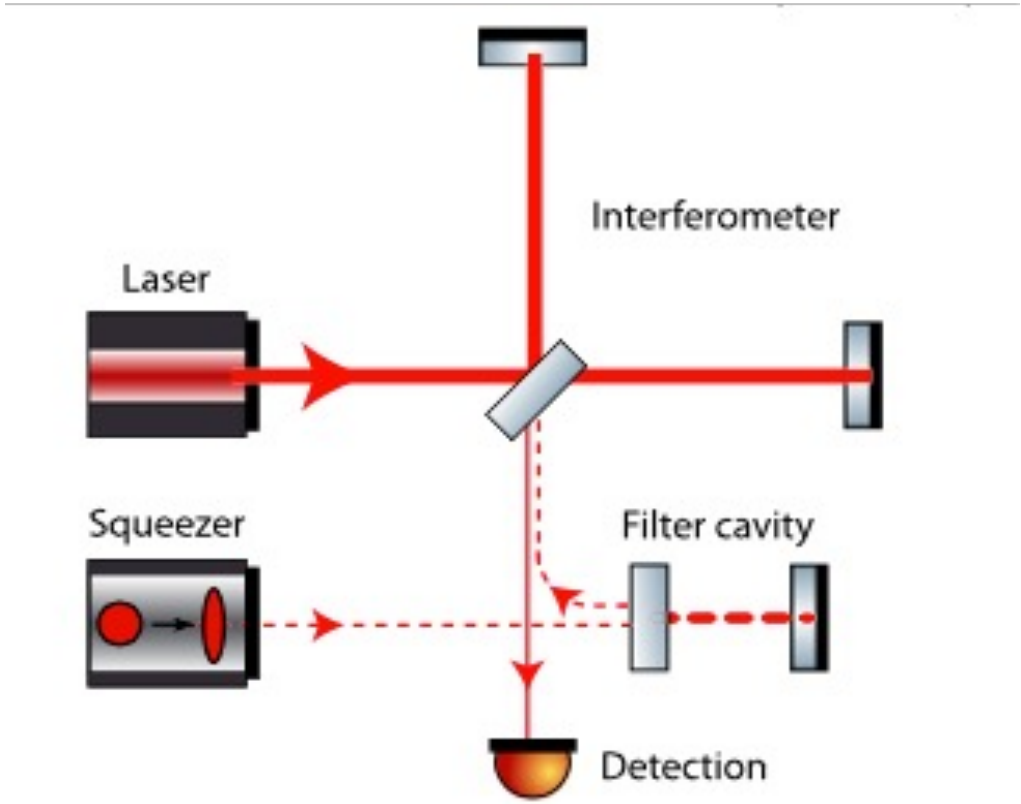

The Global GW Detector Network

Planning: a very recent update

We refer to Advanced Virgo +, but time of science run concerns the whole network

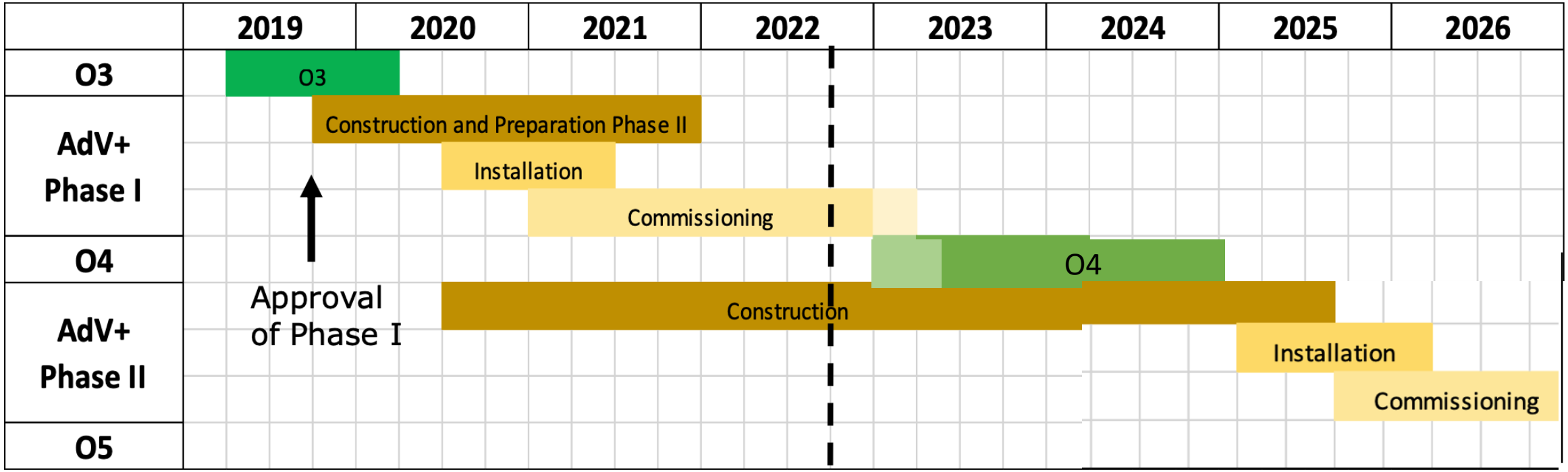

Phase I:
reduce quantum noise, hit against thermal noise. BNS range: 100 Mpc's

Phase II:
lower the thermal noise wall. BNS range: 200 Mpc's or more

GW discoveries

GW Event Catalogs: ➔ GWTC-1 ➔ 11 events , GWTC-2 (*2.1 revisited*) ➔ 55

GWTC-3 ➔90

BBH signals dominated

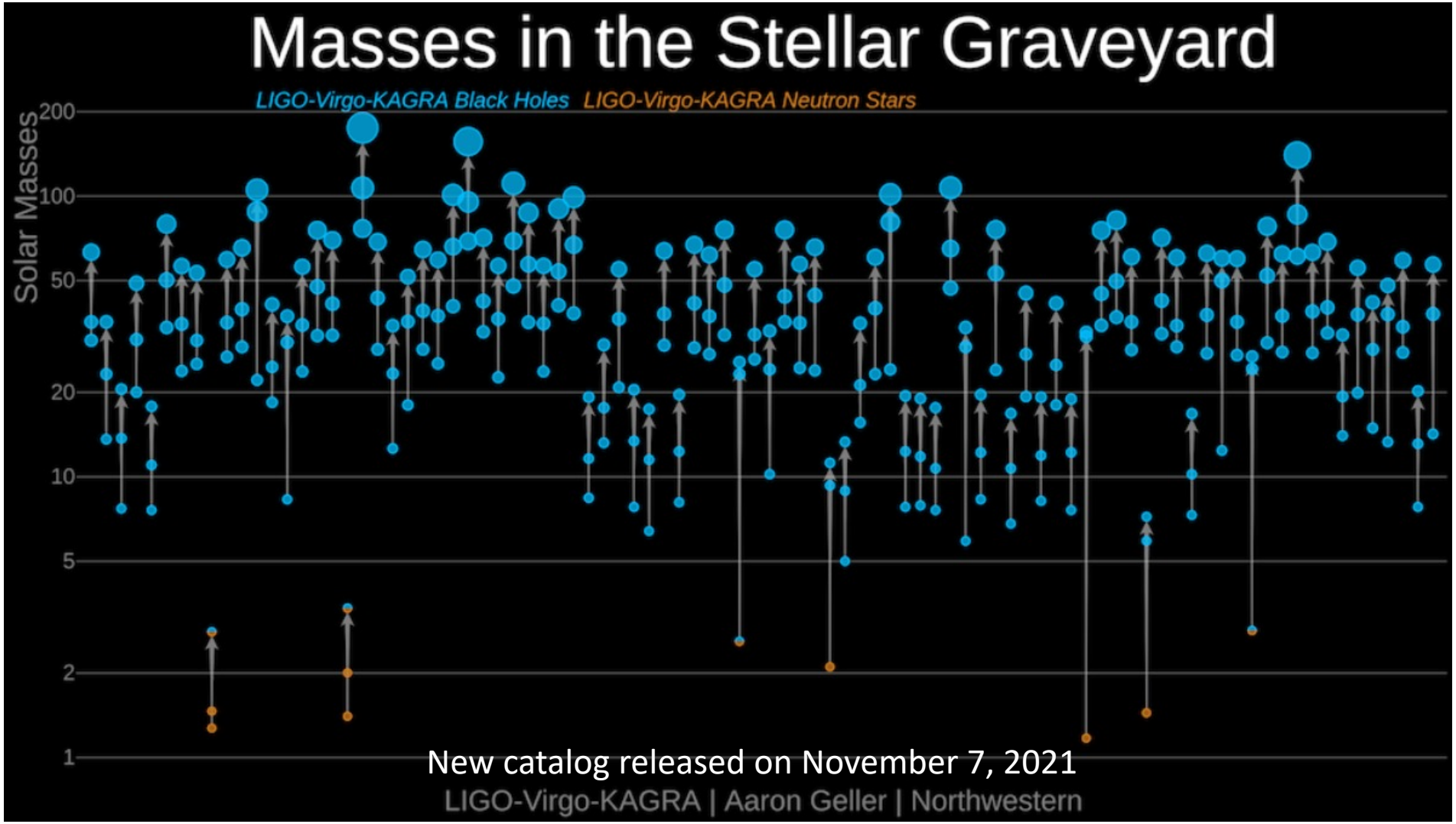

Black holes are in blue, neutron stars are in orange, and compact objects of uncertain nature in both colors. Each event is represented by three points: the two coalescing objects and the final merger remnant. (Credit: LIGO Virgo Collaboration / Aaron Geller / Northwestern).

…but we detected also NS-NS merger: GW170817

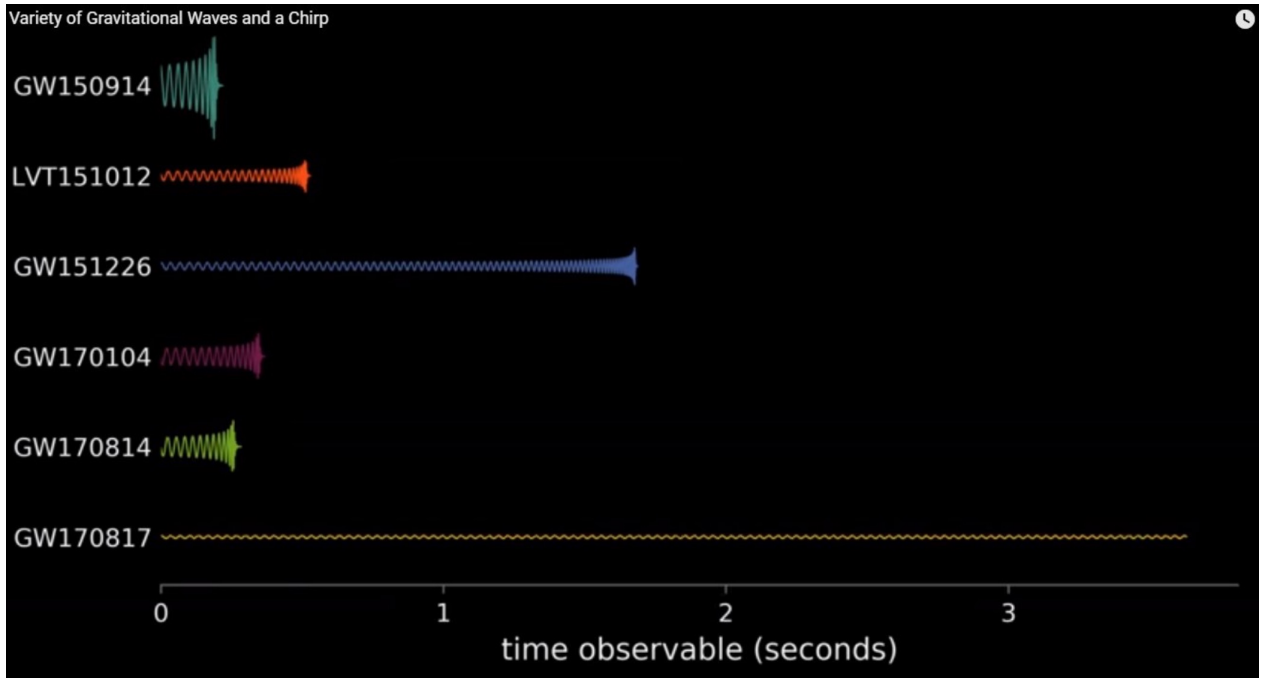

Event in NGC 4993: localisation area ~ 19 deg^2

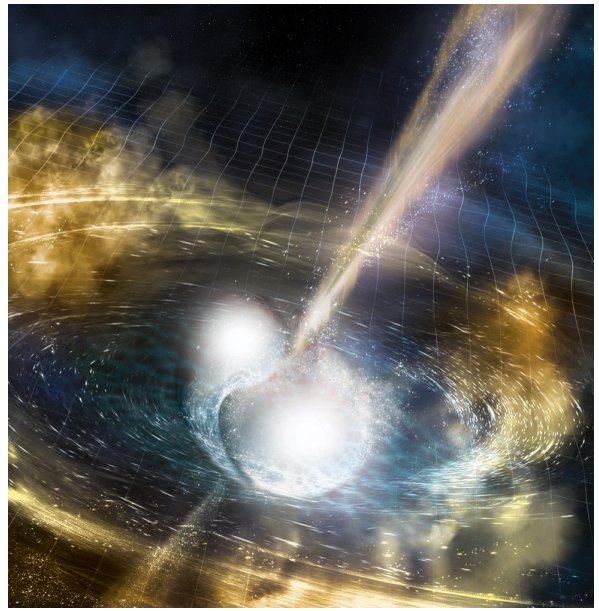

	Low-spin prior ($\chi \leq 0.05$)	High-spin prior ($\chi \leq 0.89$)
Binary inclination θ_{JN}	146^{+25}_{-27} deg	152^{+21}_{-27} deg
Binary inclination θ_{JN} using EM distance constraint [108]	151^{+15}_{-11} deg	153^{+15}_{-11} deg
Detector-frame chirp mass $\mathcal{M}^{\rm det}$	$1.1975^{+0.0001}_{-0.0001}$ M$_\odot$	$1.1976^{+0.0004}_{-0.0002}$ M$_\odot$
Chirp mass $\mathcal{M}$	$1.186^{+0.001}_{-0.001}$ M$_\odot$	$1.186^{+0.001}_{-0.001}$ M$_\odot$
Primary mass m_1	(1.36, 1.60) M$_\odot$	(1.36, 1.89) M$_\odot$
Secondary mass m_2	(1.16, 1.36) M$_\odot$	(1.00, 1.36) M$_\odot$
Total mass m	$2.73^{+0.04}_{-0.01}$ M$_\odot$	$2.77^{+0.22}_{-0.05}$ M$_\odot$
Mass ratio q	(0.73, 1.00)	(0.53, 1.00)
Effective spin $\chi_{\rm eff}$	$0.00^{+0.02}_{-0.01}$	$0.02^{+0.08}_{-0.02}$
Primary dimensionless spin χ_1	(0.00, 0.04)	(0.00, 0.50)
Secondary dimensionless spin χ_2	(0.00, 0.04)	(0.00, 0.61)
Tidal deformability $\tilde{\Lambda}$ with flat prior	300^{+500}_{-190}(symmetric)/300^{+420}_{-230}(HPD)	(0, 630)

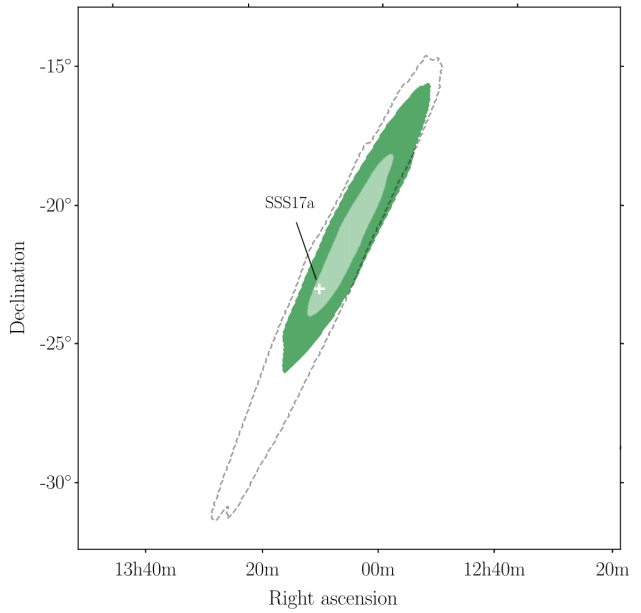

Abbott et al. Phys Rev. X 9, 011001 (2019)

Are Gravitons massless?

- GW170817 provides a stringent test of the speed of gravitational waves
- Δt =1.74 +/- 0.05 s
- $D \approx 26$ Mpc
  - Conservative limit – use 90% confidence level lower limit on GW source from parameter estimation

$$\frac{v_{GW} - c}{c} \approx \frac{c\Delta t}{D}$$

$$-3 \times 10^{-16} \leq \frac{v_{GW} - c}{c} \leq +7 \times 10^{-16}$$

Limit on Graviton mass

$$m_g < 1.76 \times 10^{-23} \text{ eV}$$

- GW170814 also puts limits on violations of Lorentz Invariance and Equivalence Principle

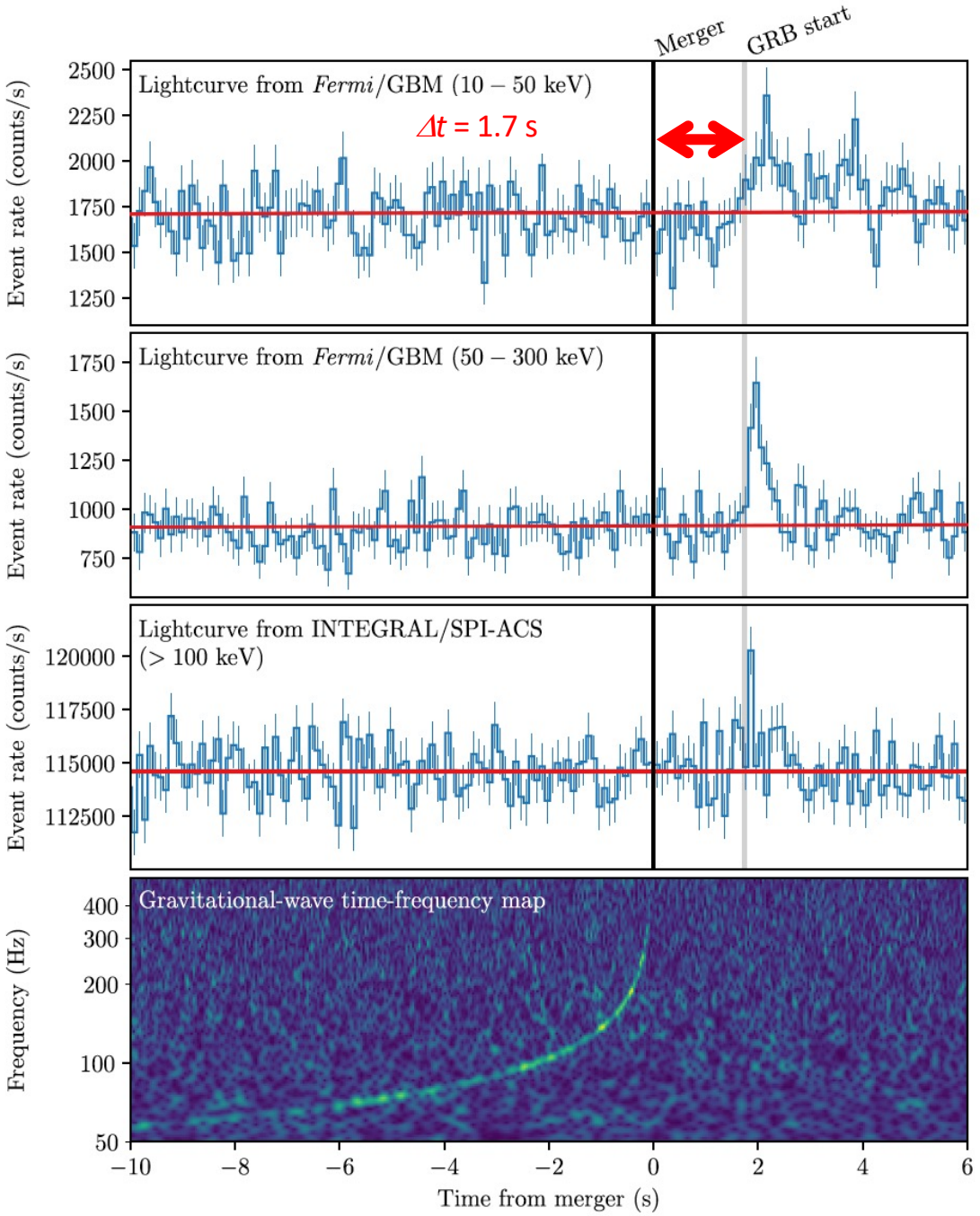

LIGO Scientific Collaboration and Virgo Collaboration, Gravitational Waves and Gamma-Rays from a Binary Neutron Star Merger: GW170817 and GRB 170817A" Astrophys. J. Lett., 848:L13, (2017)

Electromagnetic Counterparts of NS Mergers

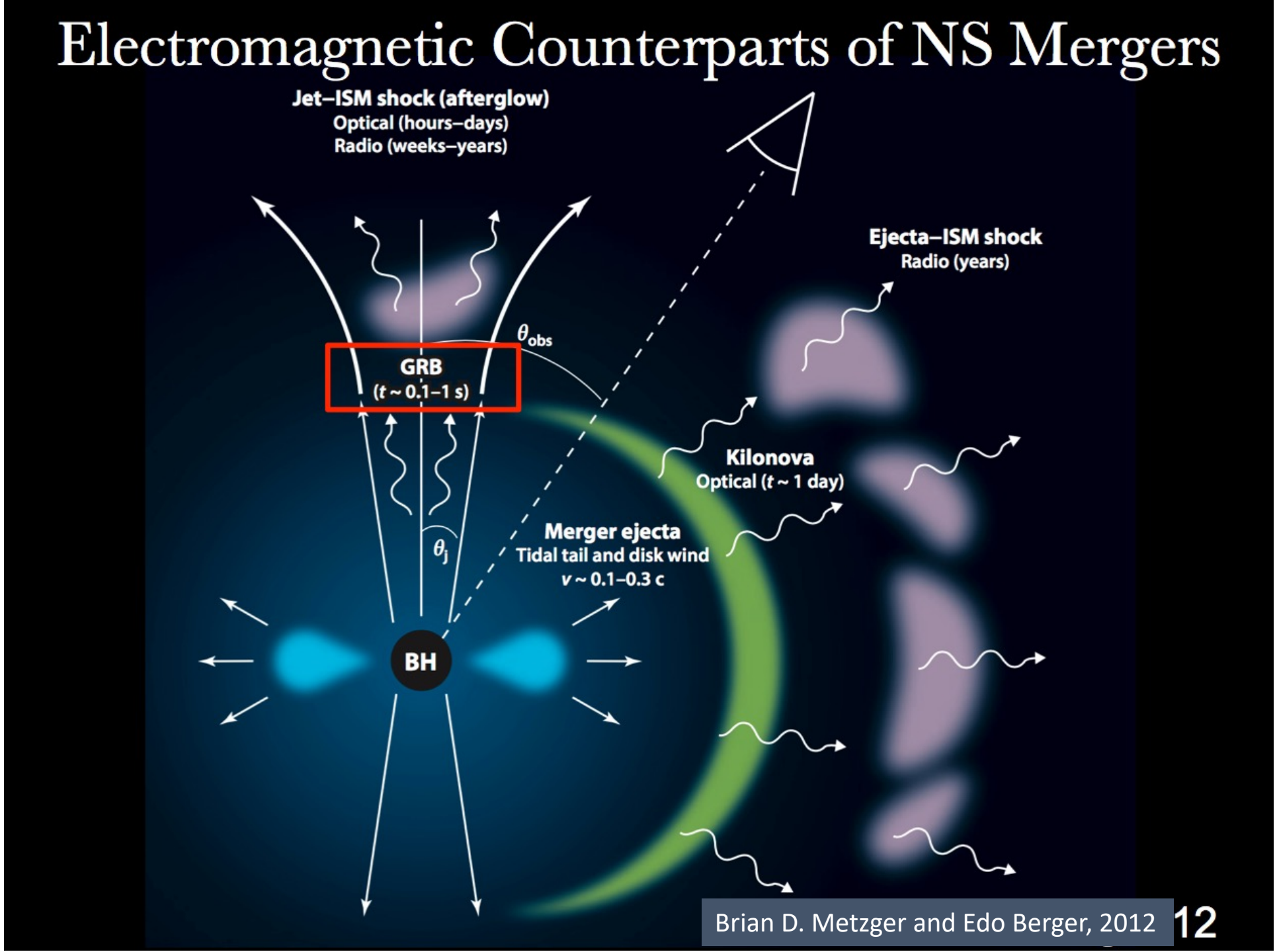

Brian D. Metzger and Edo Berger, 2012

Observations of the Kilonova across the e.m. Spectrum!

Abbott, et al. ,LIGO Scientific Collaboration and Virgo Collaboration, “Multi-messenger Observations of a Binary Neutron Star Merger” Astrophys. J. Lett., 848:L12, (2017)

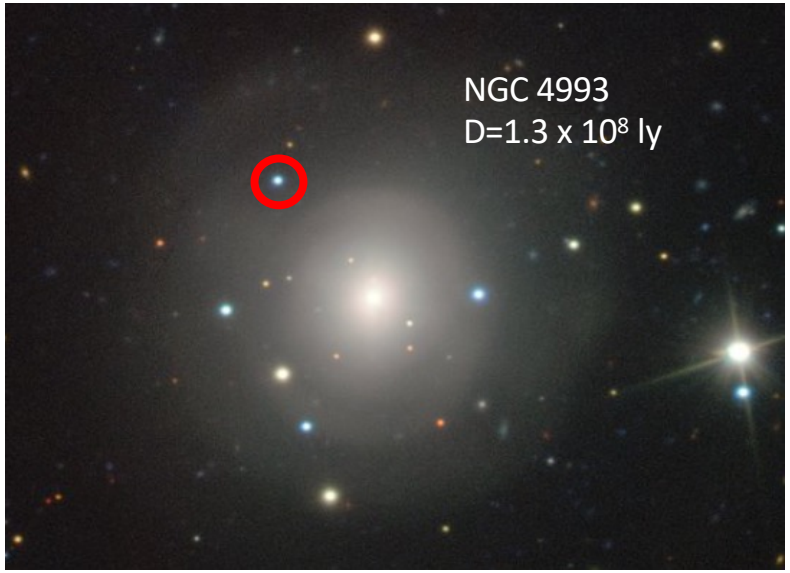

Credit: European Southern Observatory
Very Large Telescope

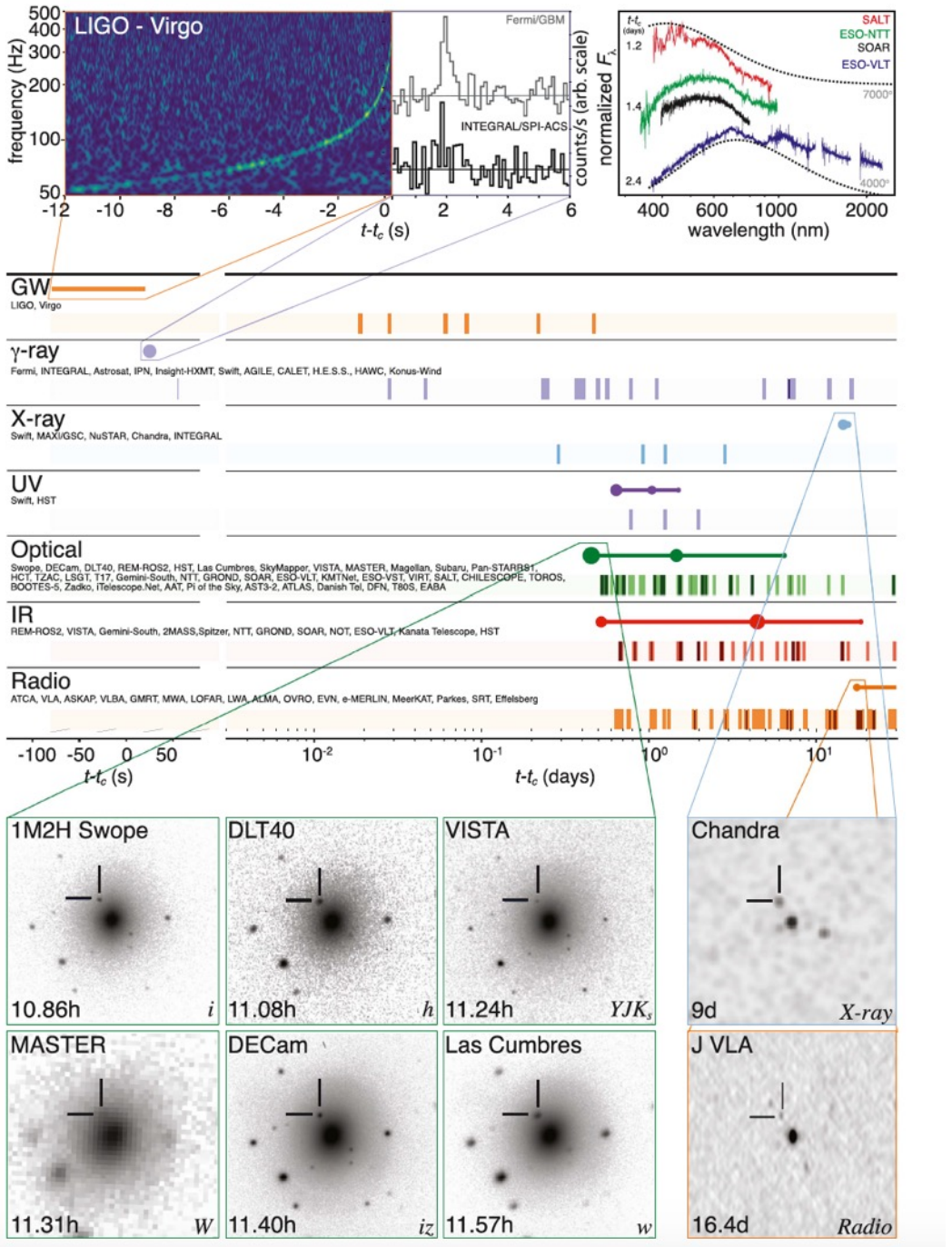

A gravitational-wave standard siren: measurement of the Hubble constant

- Gravitational waves are ‘standard sirens’, providing absolute measure of luminosity distance d_L
- can be used to determine H_0 directly if red shift is known:

$$c\,z = H_0\,d_L$$

- … without the need for a cosmic distance ladder!

$H_0 = 70\ (+12, -8)$ km/s/Mpc

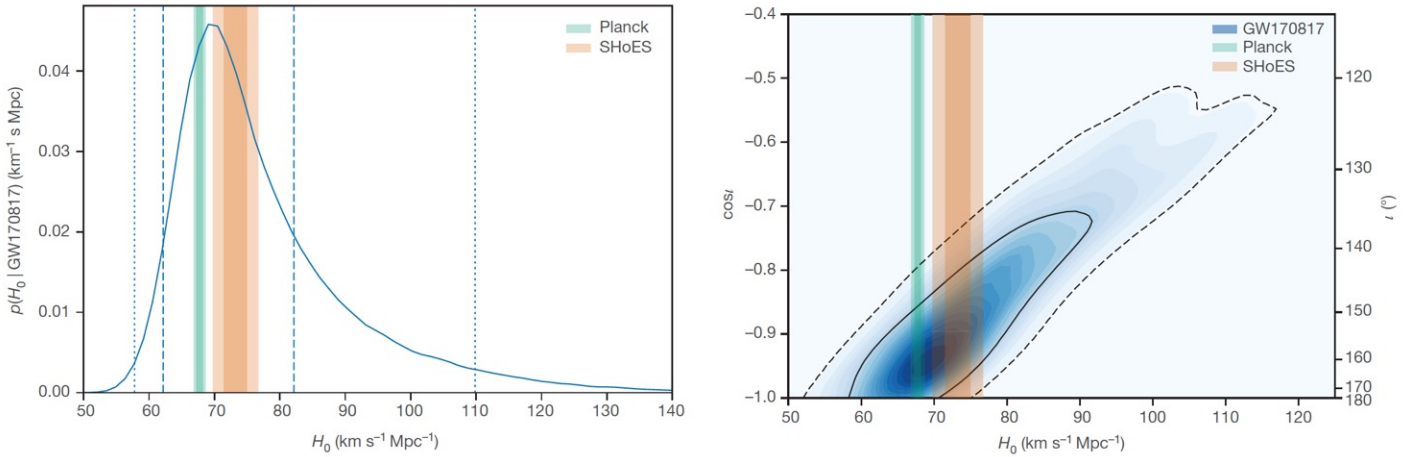

Abbott, et al., LIGO-Virgo Collaboration, 1M2H, DeCAM GW-EM & DES, DLT40, Las Cumbres Observatory, VINRO UGE, MASTER Collaborations, A gravitational-wave standard siren measurement of the Hubble constant”, *Nature* 551, 85–88 (2017).

Evidence about the synthesis mechanism of eavy elements

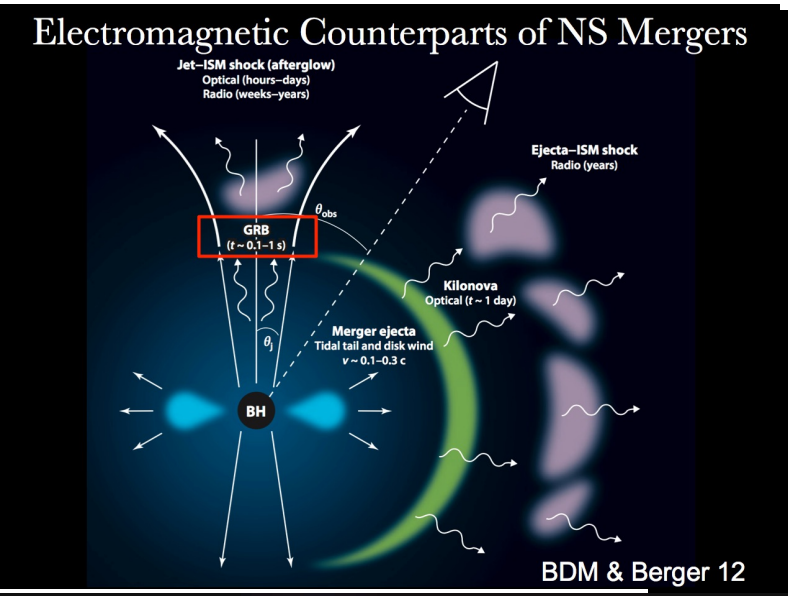

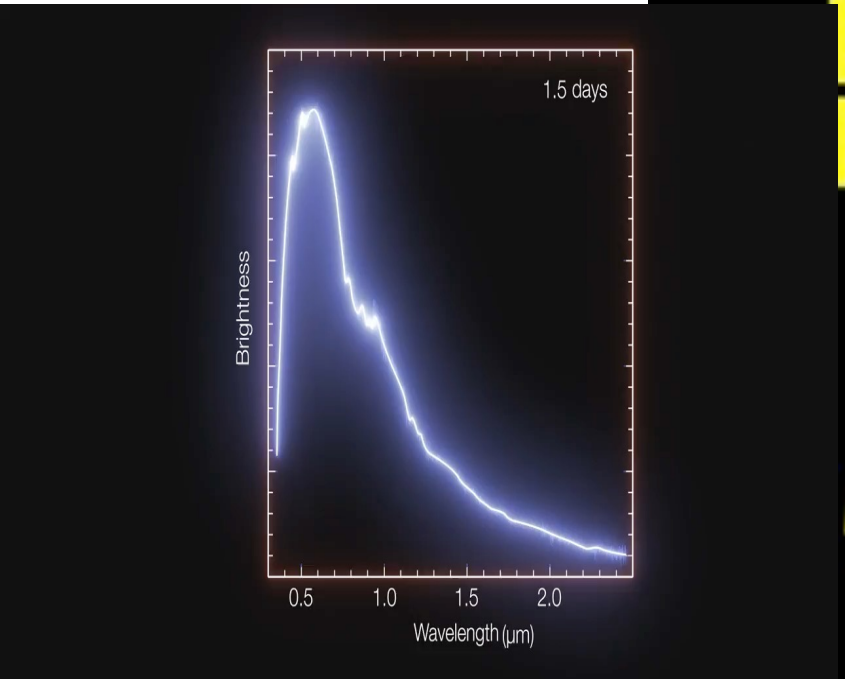

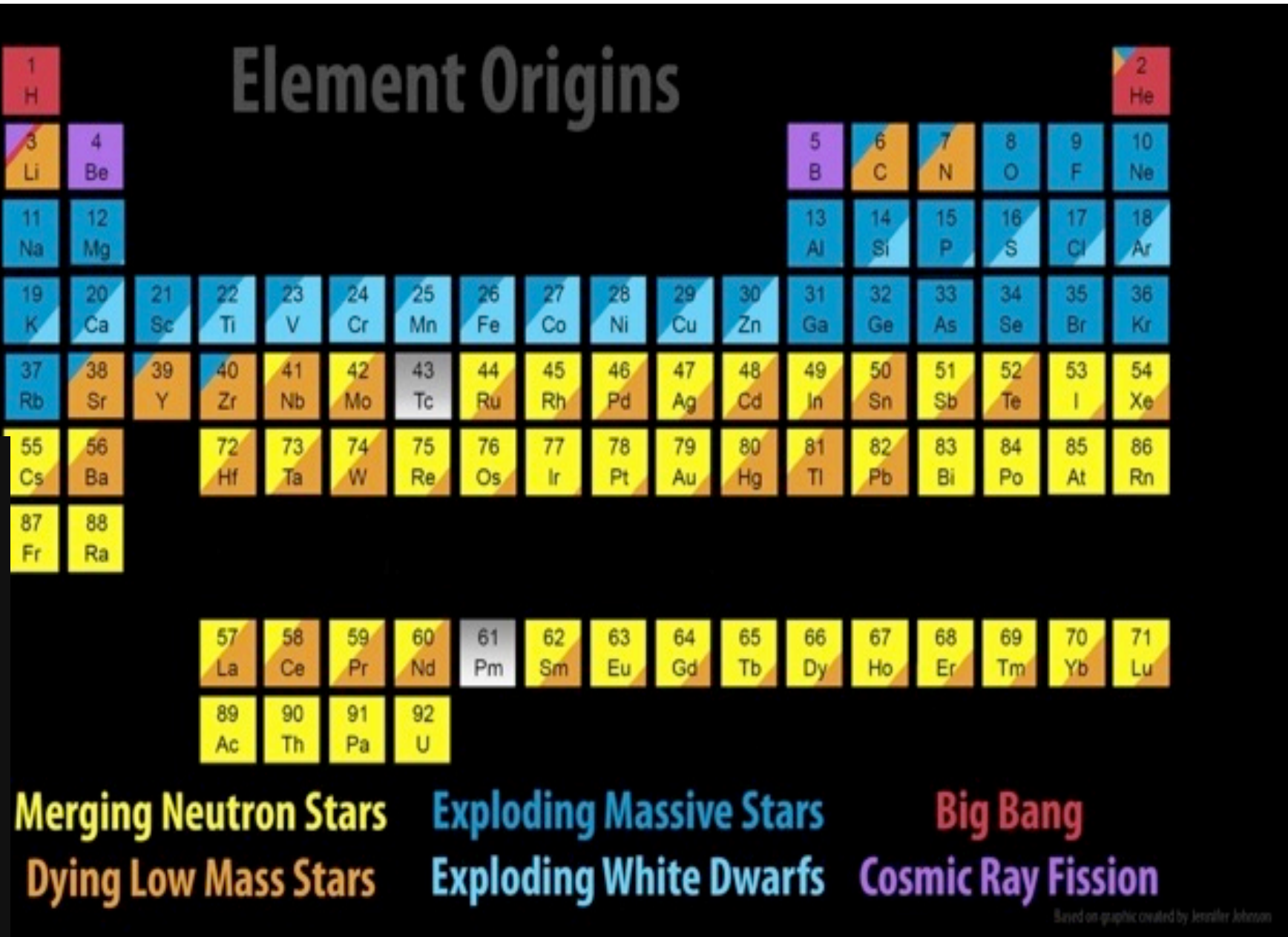

Constraining the Neutron Star Equation of State with GW170817

- Gravitational waveforms contain information about NS tidal deformations → allows us to constrain NS equations of state (EOS)
- Tidal deformability parameter:

$$\Lambda = \frac{2}{3} k_2 \left(\frac{R}{M}\right)^5$$

- GW170817 data consistent with softer EOS → more compact NS

Ozel and Friere (2016)

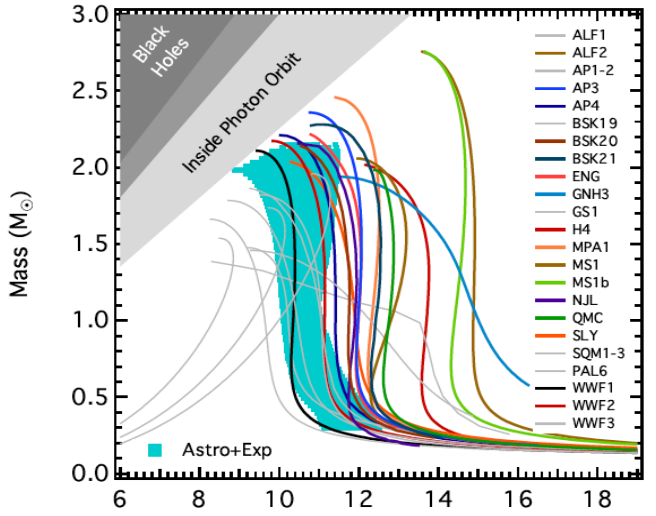

Abbott, et al. ,LIGO Scientific Collaboration and Virgo Collaboration, "GW170817: Observation of Gravitational Waves from a Binary Neutron Star Inspiral" Phys. Rev. Lett. 161101 (2017)

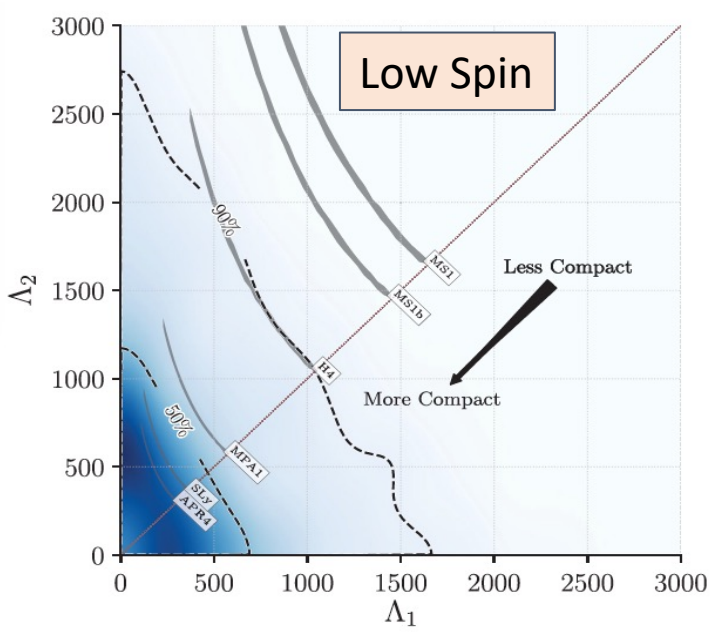

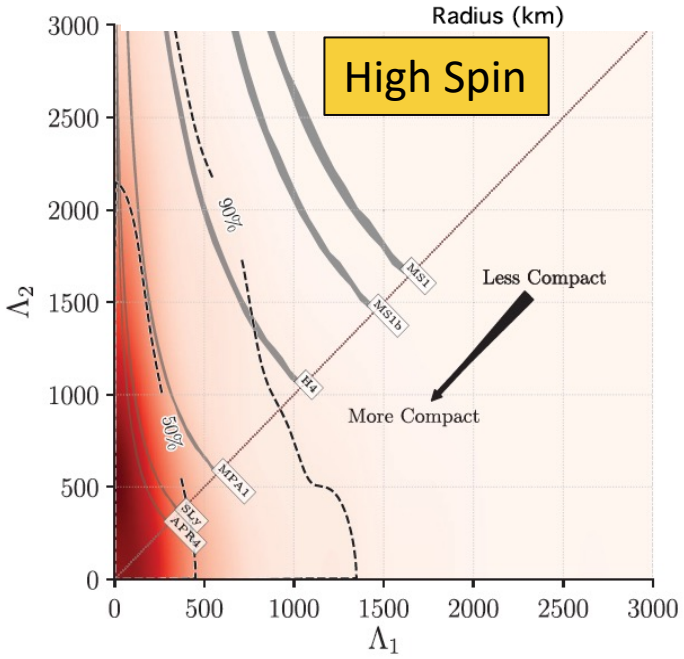

BH formation and Population Distribution

Two main scenarios of formation for stellar mass BBHs

Isolated BBH formation through common envelope

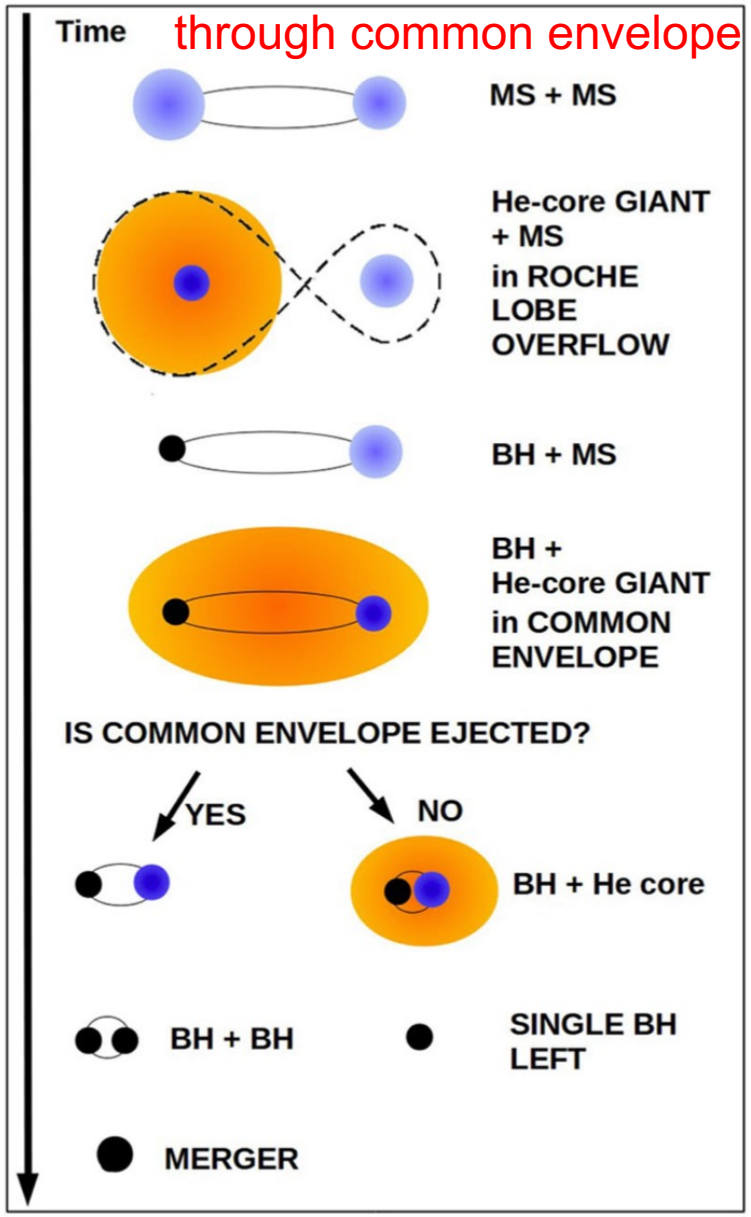

Isolated Formation

Strong gas drag from the envelope and loss of kinetic energy:

- inspiraling about each other and form a single BH
- If the envelop is ejected and the natal chick is low, BBH is formed

Dynamical Formation

During a three-body encounter, a binary star exchanges a fraction of its internal energy with the third body. If the binary is particularly tight (hard binary), such encounters tend to harden the binary star, i.e., to increase its binding energy by reducing its semi-major axis (*dynamical hardening*).

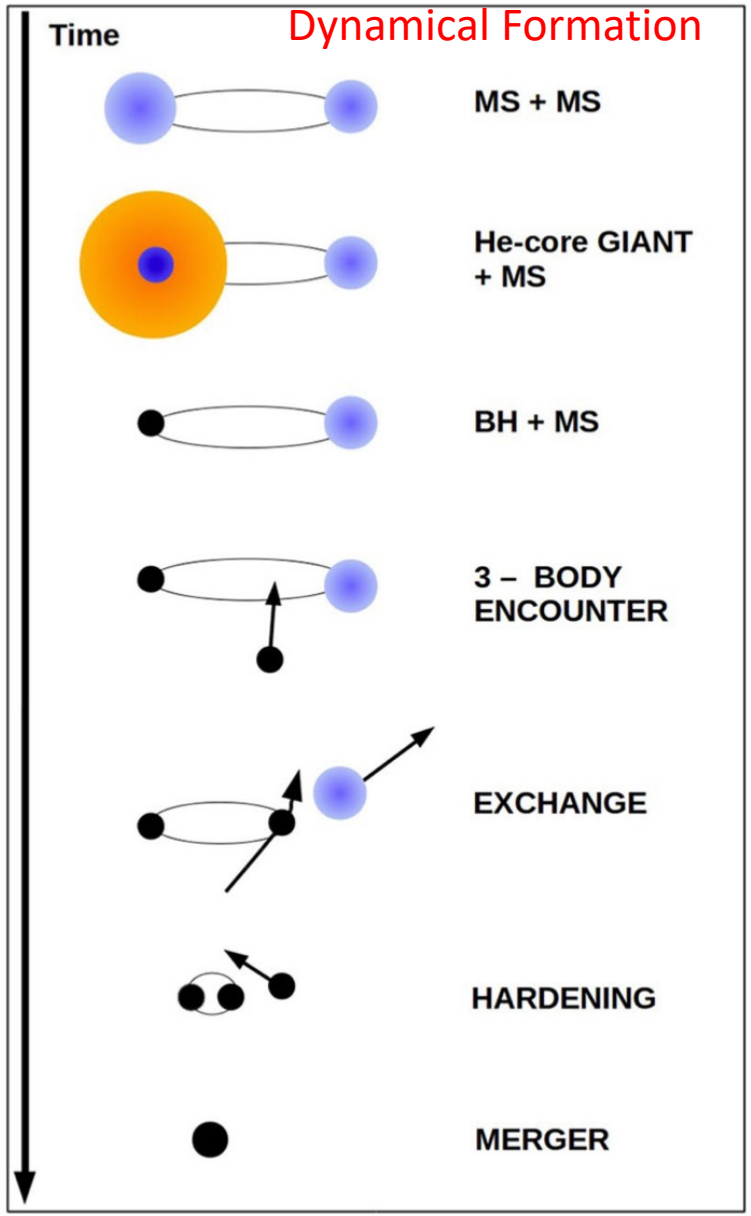

The role of the BH Spin in the Waveform analysis

Effective spin

$$\chi_{\rm eff} = \frac{\chi_1 \cos\theta_1 + q\,\chi_2 \cos\theta_2}{1+q}$$

Effective precession spin

$$\chi_{\rm p} = \max\left[\chi_1 \sin\theta_1, \left(\frac{4q+3}{4+3q}\right) q\,\chi_2 \sin\theta_2\right]$$

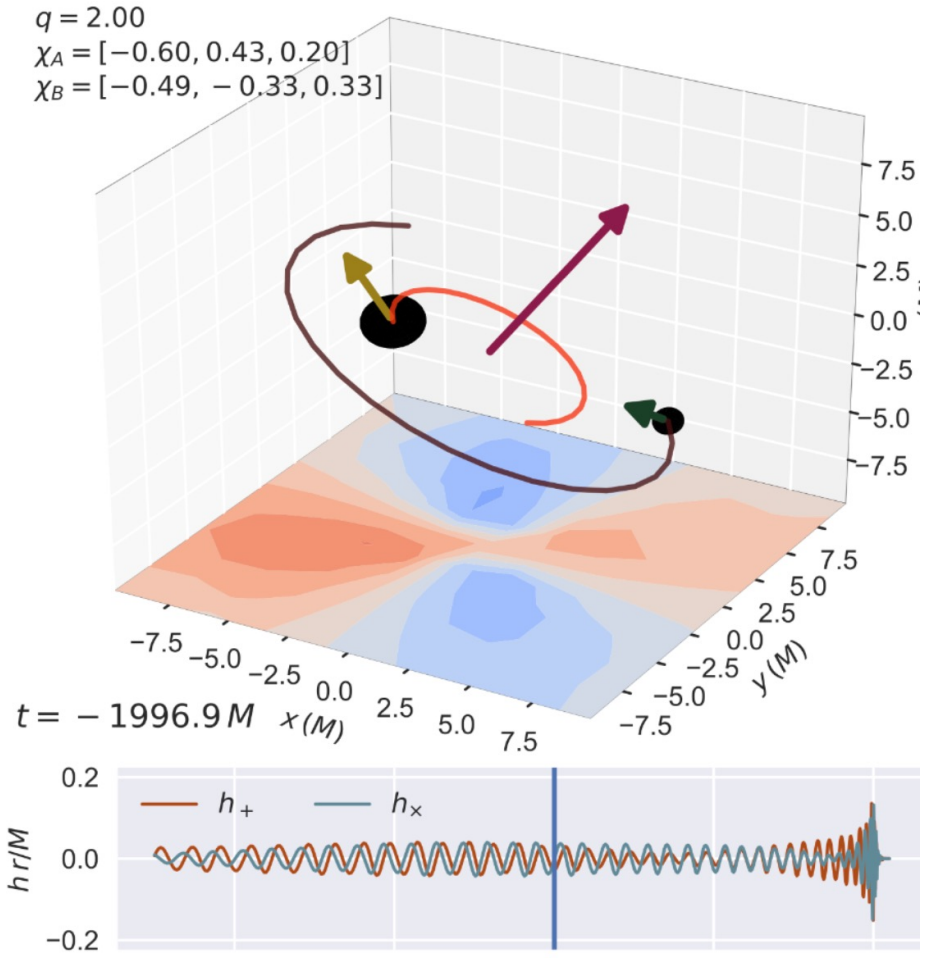

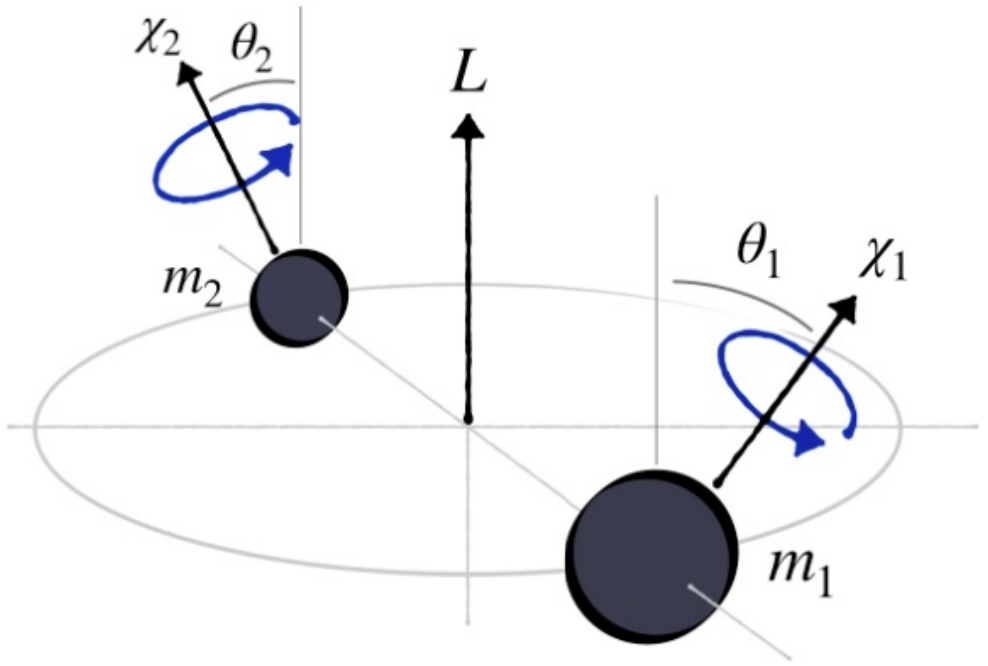

q= m_2 /m_1

Spin and hints on BH population

- BHs in dynamically formed binaries in dense stellar environments expected to have spins distributed isotropically

- BHs formed in the isolated scenario of the stellar evolution are expected to induce BH spins preferentially aligned with the orbital angular momentum

- In almost all the BBHs mergers events, the inferred probability posterior of χ_{eff} clusters around zero and is rather narrowly peaked.

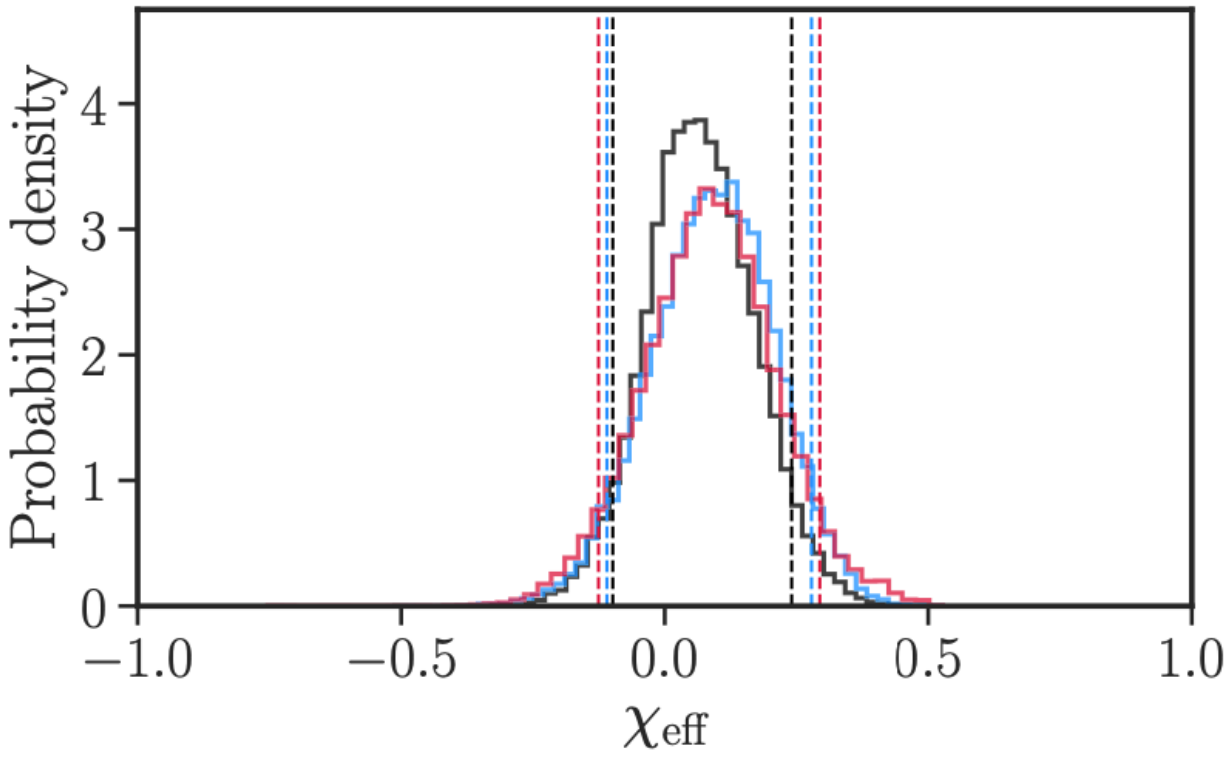

B. P. Abbott et al Phys. Rev X 9, 031040 (2019)

Simulations of stellar evolution in 11 different metallicity cases

(Astronomers use the word "metals" as a short term for "all elements except hydrogen and helium")

REM – Remenant

Mrem: Mass of the compact object

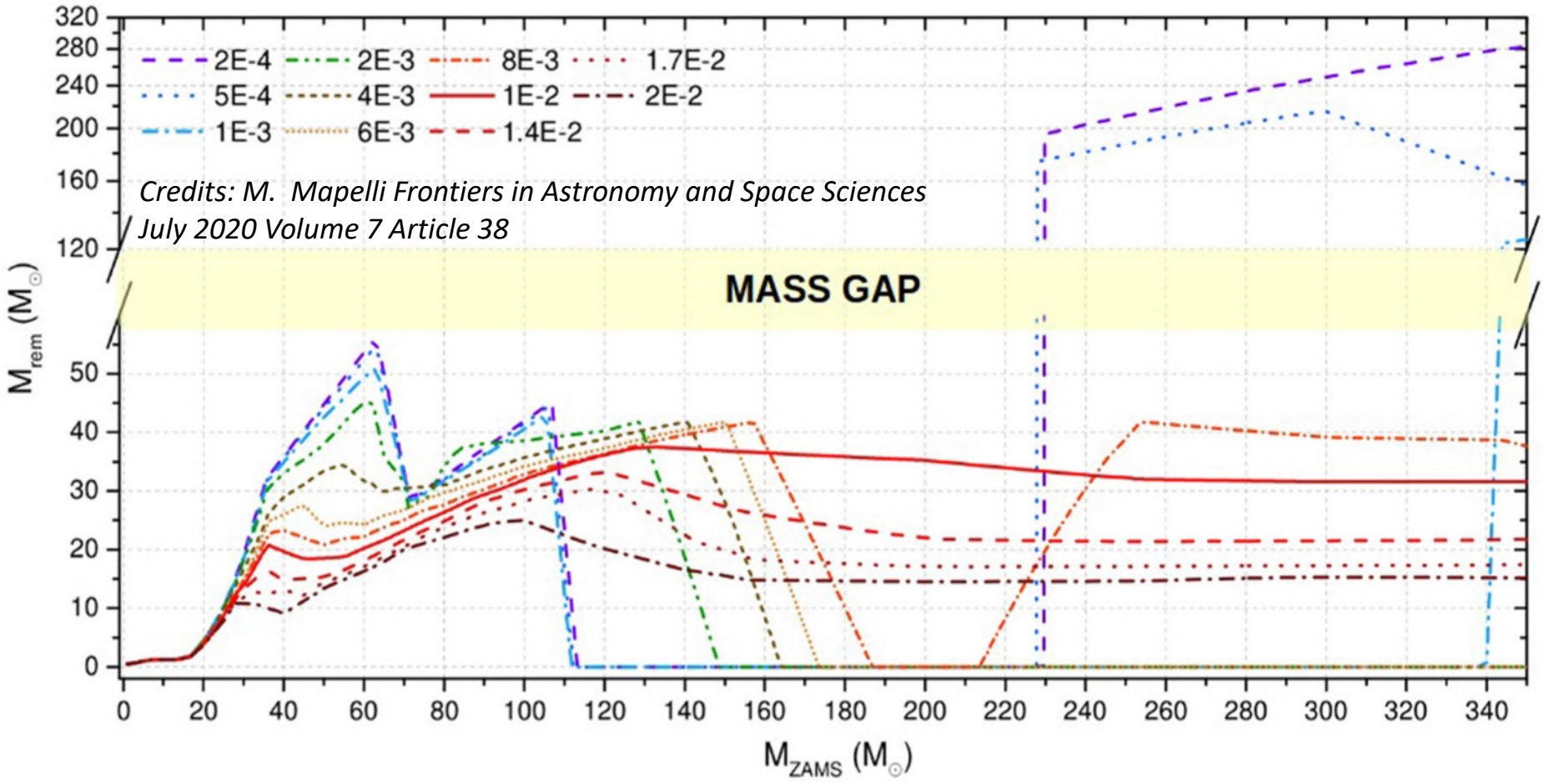

ZAMS - Zero Age Main Sequence is the is the time when a star first joins the main sequence on the Hertzsprung-Russell diagram (HR diagram) by burning hydrogen in its core through fusion reactions.

Why do they predict the existence of a mass gap ?

The model

- In stars with a main-sequence mass of approximately 150 $M_{\odot}$–260 $M_{\odot}$, the conversion of photons to e^+ / e^- pairs inside the hot dense core drives a runaway collapse.
- *When this collapse is halted by oxygen-burning nuclear reactions, the energy produced leads to an explosion powerful enough to completely destroy the star. The Supernova dominated by the pair instability mechanism do not leave any BH remnant.*
- Conclusion: the stellar evolution model tells us that there should be no black holes with masses in the range 50 $M_{\odot}$–140 $M_{\odot}$

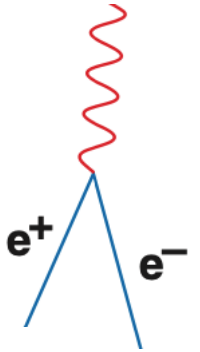

Data from LIGO/Virgo

- GW190521 LIGO/Virgo event results from a BBH merger of black holes with masses of 66 $M_{\odot}$ and 85 $M_{\odot}$
- *At least one of the two BHs is well in the mass gap challenging the pair instability model.*

Attempts to conciliate model and data

- It is possible to move the boundaries of the mass gap by including rotation or magnetic fields in the calculation, but physically reasonable values of these seems not to permit that isolated stars populate the mass gap. (*D. Branch and J.C. Wheeler, Supernova Explosions, - Springer, New York, 2017*)

- If an energy source is added throughout the star in addition to nuclear fusion, it is possible to end up with a BH remnant: *J. Ziegler and K. Freese suggest as additive mechanism the case of dark matter annihilation (Phys. Rev. D 104, 043015 (2021)*

GW190814 and its ‘mystery object’

LVC, Astrophys.J.Lett. 896 (2020) 2, L44

Primary Object a BH of ~23 $M_\odot$,

Secondary Mass 2.50 -2.67 $M_\odot$:
a super-heavy NS or a super-light BH

Outlier in secondary mass & mass ratio distributions:
Probability <0.02% of seeing *as small* a m_2 (or low $q=m_2/m_1$) over 45 events

Indicates potential origin different from the majority of BBH detected up to now

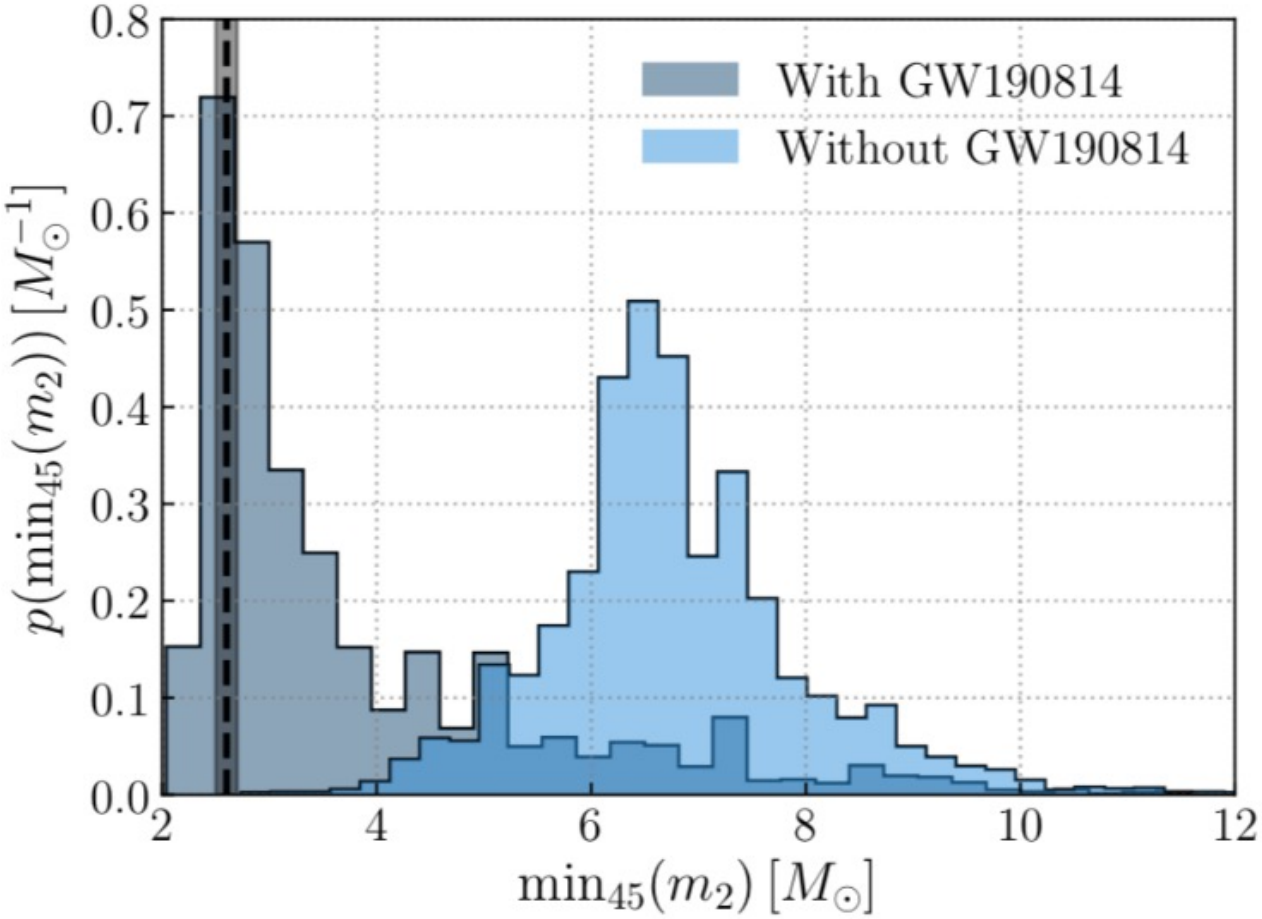

Primordial BH contributing to the Dark Matter - DM

PBH could have formed deep in the radiation era of the Universe from the prompt collapse of large primordial over-densities on the scale of the early time Hubble volume

If the limits set by micro lensing observation are correct, the PBH contribution to DM should be limited to BH masses below 1 $M_{\odot}$

Limit on the PBHs lighter than $\sim 10^{15}$ g have been computed also considering:

- the abundance of the light elements produced by the big bang nucleosynthesis (10^{9} g < M_{PBH} < 10^{13} g),
- the extragalactic photon background (10^{14} g < M_{PBH} < 10^{15} g),
- the damping of the CMB temperature anisotropies on small scales by modifying the cosmic ionisation history (10^{13} g < $M_{P\,BH}$ < 10^{14} g).

To date, no PBH detection with GW signals has been made so far !

Upper limit on the fraction of DM in BH of mass 0.2 - 1.0 $M_{\odot}$ **< 16%**

Abbott B. P. et al. Search for subsolar mass ultracompact binaries in ad- vanced LIGO's second observing run. Phys. Rev. Lett. 123, 161102 (2019)

Black Hole and Fundamental Physics

Vitor Cardoso, Paolo Pani
Testing the nature of dark compact objects: a status report
Living Reviews in Relativity (2019) 22:4

Marco Giammarchi, Fulvio Ricci
Gravitational Waves, Event Horizons and Black Hole Observation: A New Frontier in Fundamental Physics
Symmetry 2022, 14(11), 2276

Short Recap on BH Physics

General Relativity and BH:

- Schwarzschild prediction (1916) horizon radius $R_S = 2\,G\,M/c^2$
- No hair therorem.
  - a stationary black hole, as predicted by the Einstein–Maxwell equations of GR + e.m. theory are characterized just by mass M, electric charge Q and angular momentum . Other characteristics (such as geometry and magnetic moment) are uniquely determined by these three parameters

Example of a simple consequence: two BHs with the same M, Q and J, one made of anti-matter, the other made of matter are indistinguishable.

- GR BH + Quantum Mechanics ➔ Bekenstein –Hawking Thermodynamics
  - BHs are more than simple geometrical objects. A distant observer sees a thermal distribution of particles emitted at a finite temperature*: Hawking radiation*
  - Entropy ➔ $S(M, \chi) = k_B\, A/(4\, l_P^{\,2}) = 2\pi k_B (M/m_P)^2 [1+(1-\chi)^{1/2}]$ ($Q=0$, $\chi = [\,c\,J\,/\,(G\,M^2)\,]$
  - *Hawking temperature* ➔ $T = (h\,c^3)\,/\,(16\,\pi^3\,k_B\,G\,M)$

BH open questions

- How well are these black holes described by General Relativity, and will new physics eventually be required, perhaps involving a quantum theory of gravity?

The information paradox

Applying QM, Hawking argued that the radiation associated to the BH evaporation depend only on BH mass, electric charge and angular momentum Since many different states can have the same mass, charge and angular momentum this suggests that many initial physics state could evolve into the same final state. **Thus, information about the details of the initial state would be permanently lost.**

Violation of unitarity principle: the state of a system at one point in time should determine its value at any other time

Information paradox is an active field of research within Quantum Gravity

BH themodynamics as bridge between GR and QM

- Thermodynamics of the equilibrium states is a macroscopic description of an ensemble of many microscopic states, corresponding to the different possible ways of forming the same macroscopic solution.
- Enumerating these microstates we can derive the laws of thermodynamics from the kinetic theory of gases

- BH entropy and temperature are intrinsically related to the quantum nature of the system, but are related to macroscopic quantities: horizon area and surface gravity as provided by GR.

- Starting from a fundamental theories of Quantum Gravity, in an appropriate average limit, should permit to derive BH Thermodynamics.

The thermodynamic behaviour of BHs gives insights into the nature of quantum phenomena occurring in strong gravitational fields.

Spin population , BH Thermodynamics and GW data

Bianchi et al. arXiv:1812.05127v

Probability to find a spin a in a fixed microcanonical ensemble of mass M is

$$P_M(\chi) = \chi^2 \, e^{S(M,\chi)} / N$$

N ➔ normalization factor and $S(M, \chi) = k_B A/(4 l_P^2) = 2\pi k_B (M_i/m_P)^2 [1+(1-\chi)^{1/2}]$

For equal masses (M), higher spins (χ) correspond to lower entropy values, i.e. we should have fewer microstates with large spin than with small spin.

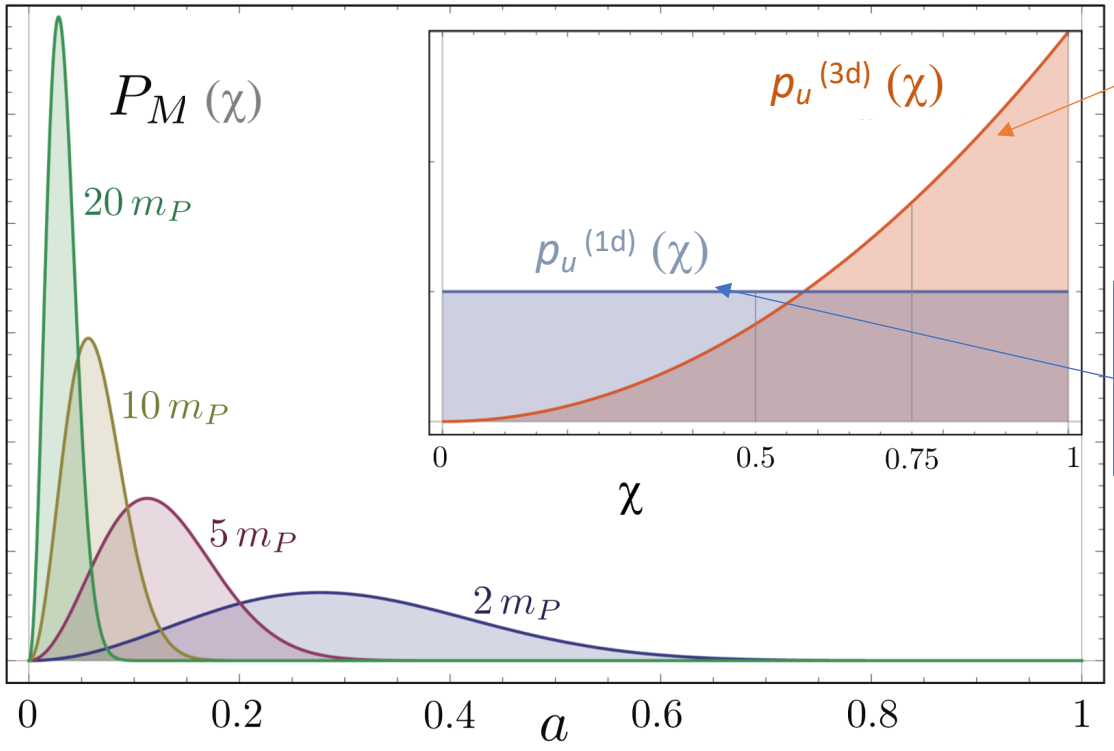

A first attempt to compare data with the spin distribution computed on the base of P(χ) derived assuming the microcanonical ensamble formula

Bianchi et al. arXiv:1812.05127v

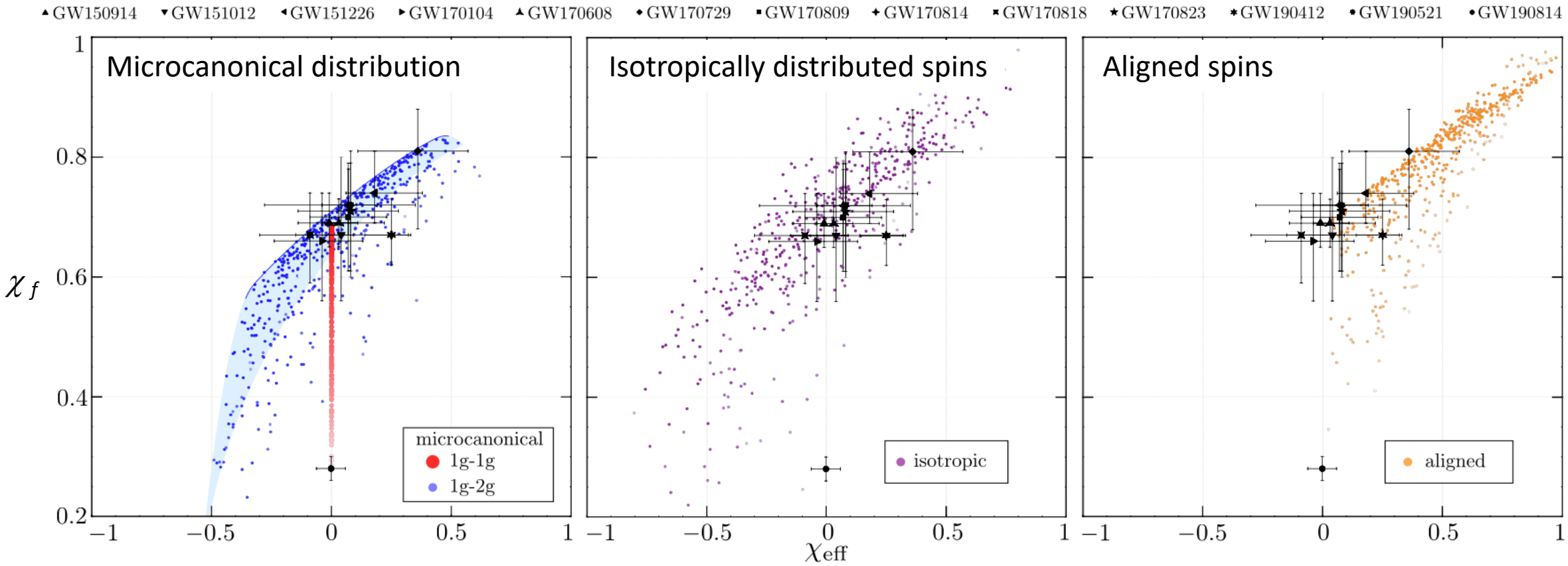

BH formation modeling

- 1g => BH of first generation,
- 2g => BH of second generation

Test of the Bekestein-Hod bound on BH information loss

- Bekenstein derived an universal bound for the maximum average rate of information emission achievable by a physical system
- Hod noted that this bound applies to the ring-down phase of a BH relaxing towards equilibrium. He quantified the bound by introducing the information loss parameter $\mathcal{H}$, a quantity having an explicit dependence on the relaxation time of a perturbed black hole $\tau = 1/\omega_I$ and the BH temperature T

$$\mathcal{H}_{max} = \frac{1}{\pi}\frac{\hbar\omega_I}{k_B T} \leq 1$$

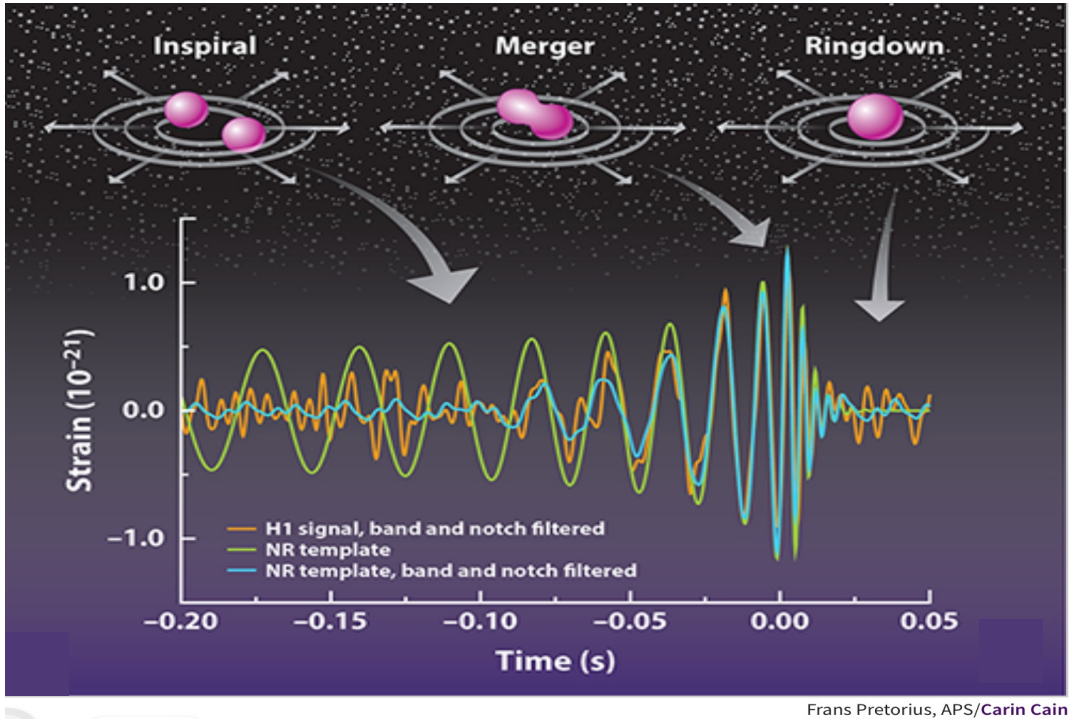

Frans Pretorius, APS/Carin Cain

Using a time-domain ringdown analysis of BBH events of GW catalogue of signals the Bekenstein-Hod bound has been verified

See CarulloG.,LaghiD.,VeitchJ.,DelPozzoW.,B□ekenstein-HodUniversalBoundonIn- formation Emission Rate Is Obeyed by LIGO-Virgo Binary Black Hole Remnants Physical Review Letters 126, 161102 (2021)

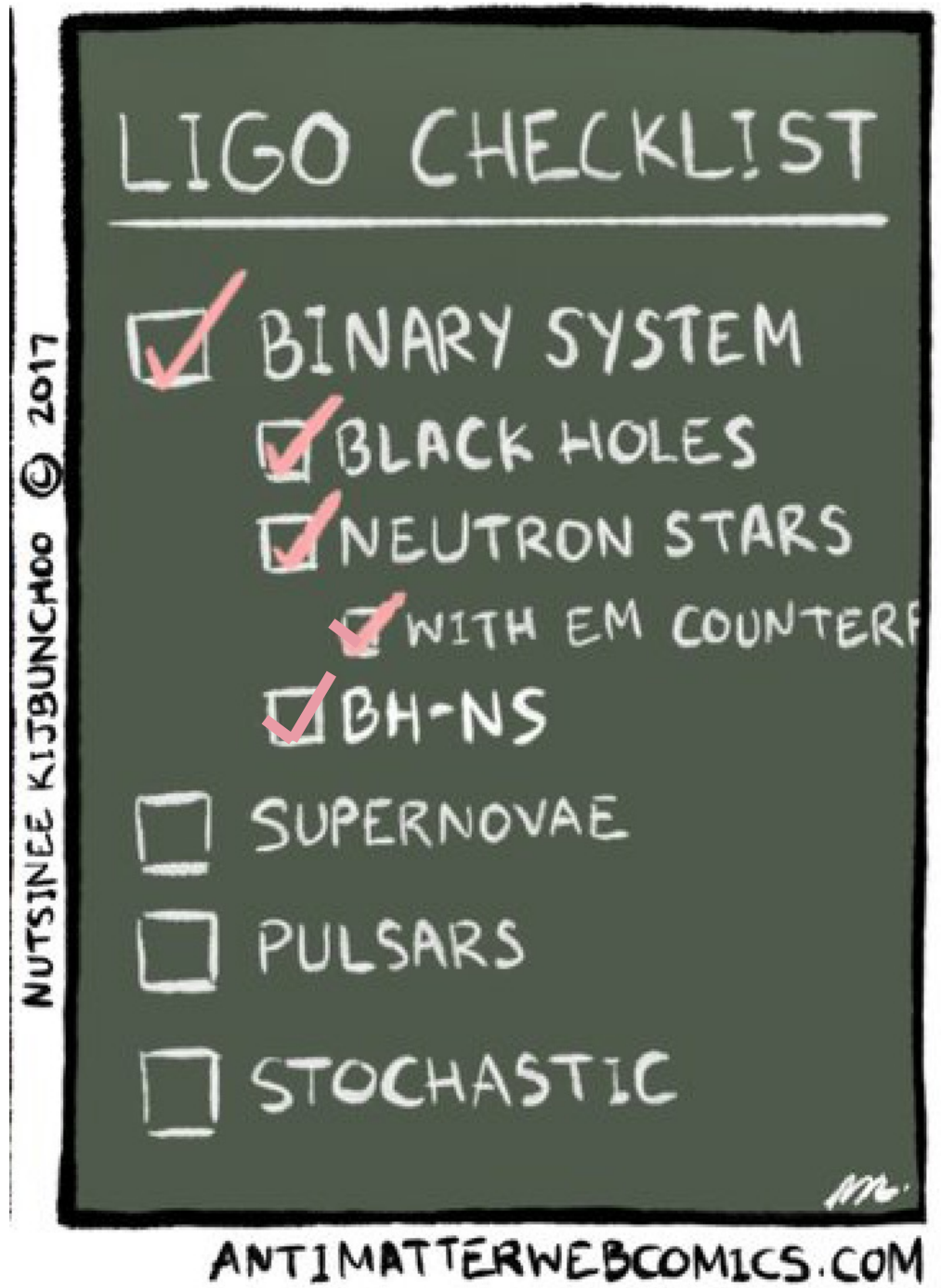
LIGO CHECKLIST
BINARY SYSTEM
BLACK HOLES
NEUTRON STARS
WITH EM COUNTERP
BH-NS
SUPERNOVAE
PULSARS
STOCHASTIC
NUTSINEE KIJBUNCHOO © 2017
ANTIMATTERWEBCOMICS.COM

Core Collapse SuperNovae - CCSN: the holy grail of multimessenger astronomy

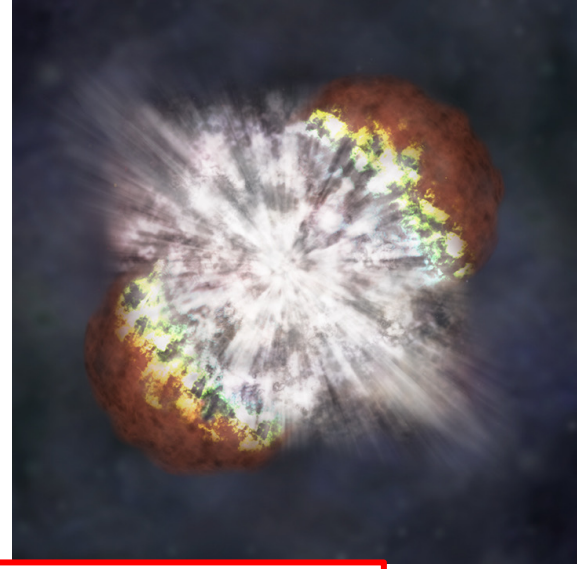

Target: detection of GW emitted by a CCSN event in our galaxy (several/century)

$$h_{ij} = \frac{2G}{c^4 R}\frac{\partial^2}{\partial t^2}Q_{ij} \sim \varepsilon \frac{R_s}{R}\left(\frac{v}{c}\right)^2$$

ε ➔ degree of anisotropy

$R_s = 9.7 \times 10^{-17}$ kpc $(M/M_\odot)$

$v/c \sim 0.1$ $R \sim 10$ kpc $M/M_\odot \geq 10$ $\varepsilon \sim 10^{-2}$

$h \sim 10^{-20}$

GW signal structure predicted on the base of 3D simulations: huge computational challenge!

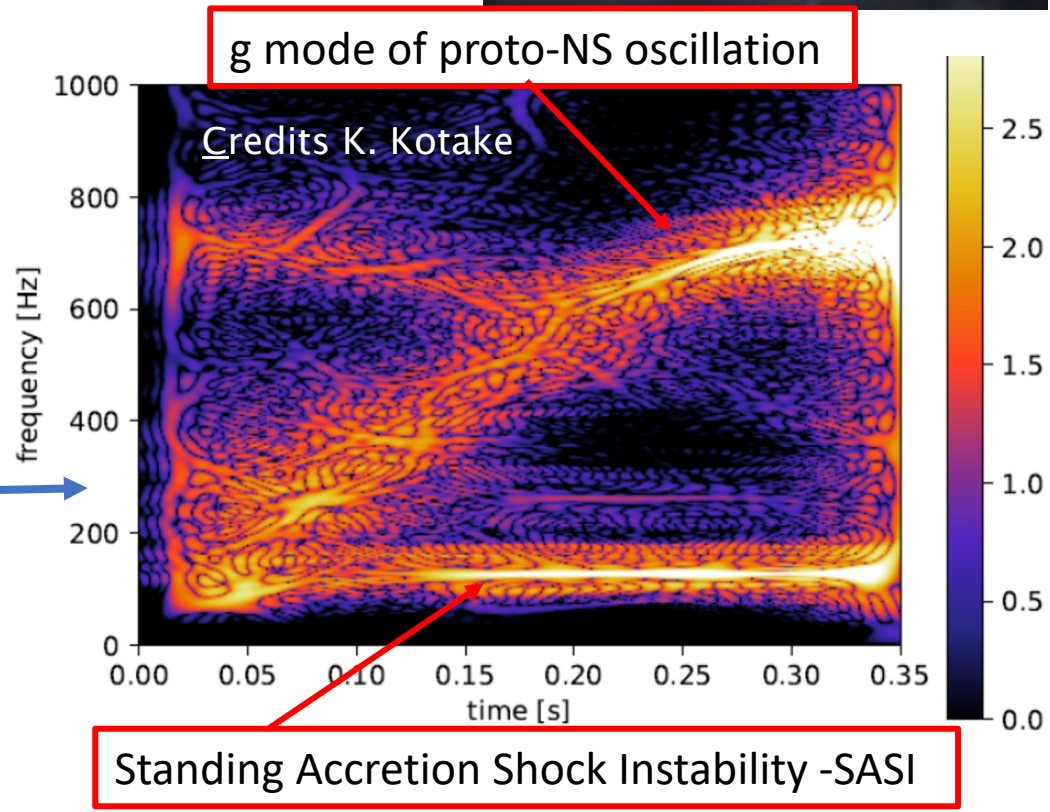

P. Astone, P. Cerdá-Durán, I. Di Palma, M. Drago, F. Muciaccia, C. Palomba, and F. Ricci ; *New method to observe gravitational waves emitted by core collapse supernovae* Phys. Rev. D 98, 122002(2018)

M. López, I. Di Palma, M. Drago, P. Cerdá-Durán, and F. Ricci
Deep learning for core-collapse supernova detection
Phys. Rev. D 103, 063011 (2021)

Correlation of ν and GW signals from a rapidly rotating 3D model

Takiwaki, KK, Foglizzo, (2021)

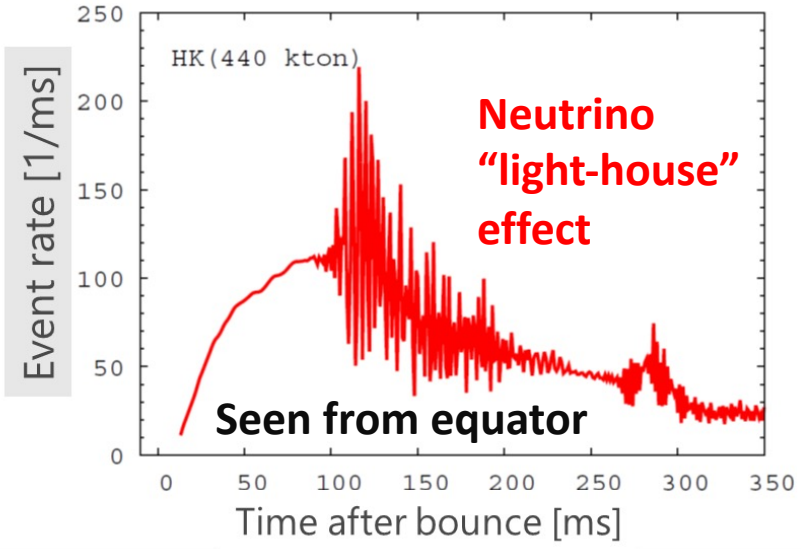

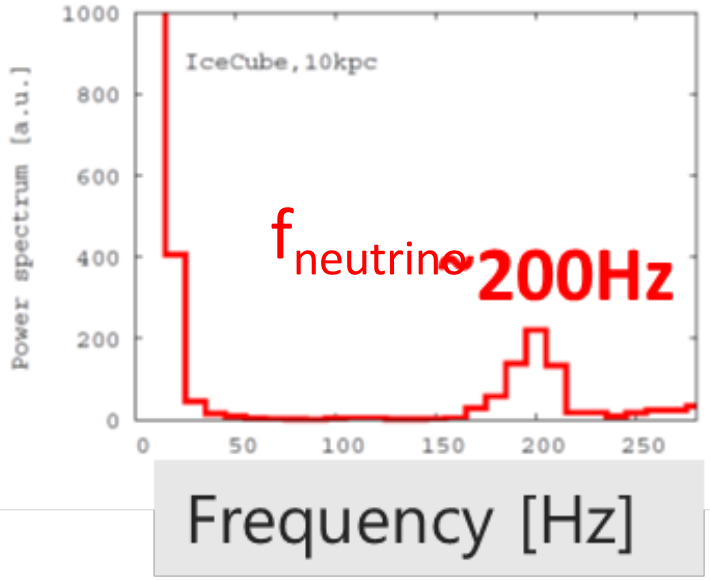

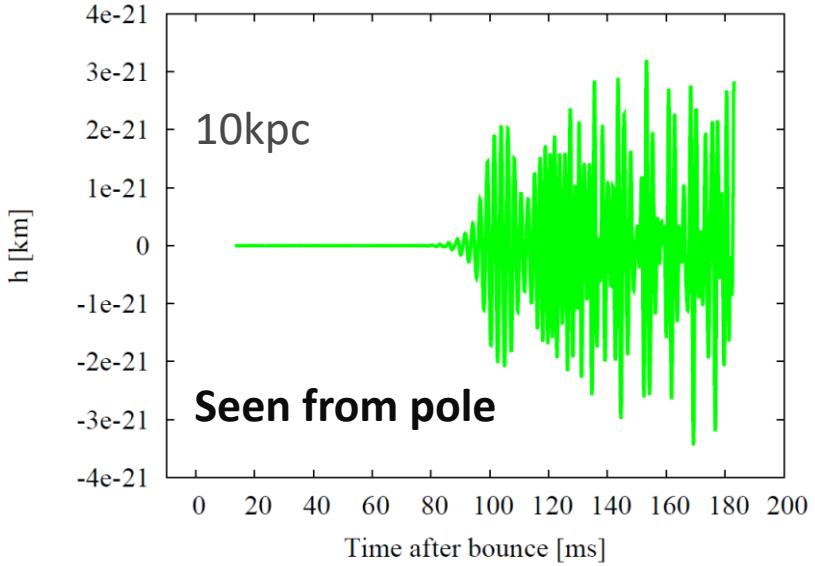

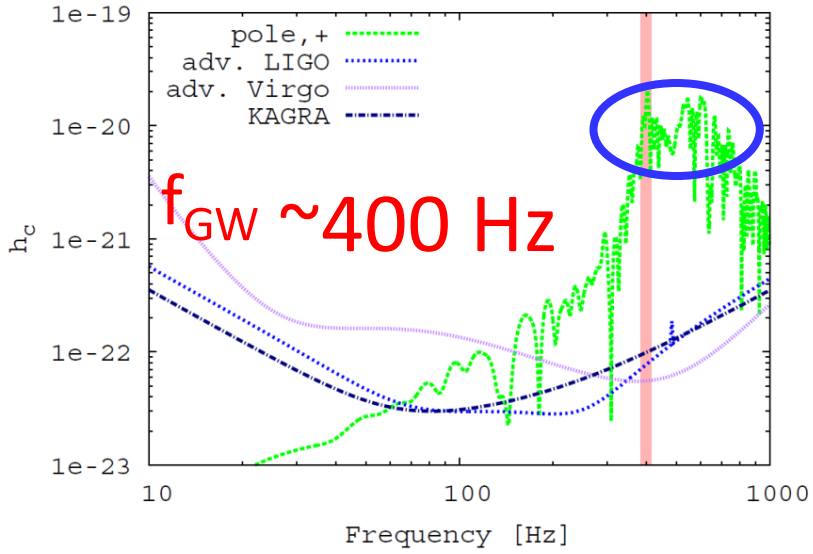

Neutrino event rate (27 M_{sun}, Ω_0 = 2rad/s)

Credits: Kei Kotake

- ✓ Peak frequency of the GW signal twice of the neutrino modulation (due to the quadrupole GW emission)
- ✓ Also the case for non-rotating progenitore $f_{neutrino,SASI}$~ 80 Hz , f_{gw} ~ 80 or160 Hz
- ✓ Concident detection between GW and ν : smoking gun signature of rapid core rotation!

Next Challenge: continuous GW waves

Continuous gravitational waves produced by systems as:

- binary sytems of stars or black holes orbiting each other (long before merger),
- Neutron Star (NS) swiftly rotating about its axis with a mountain or other irregularity on it.

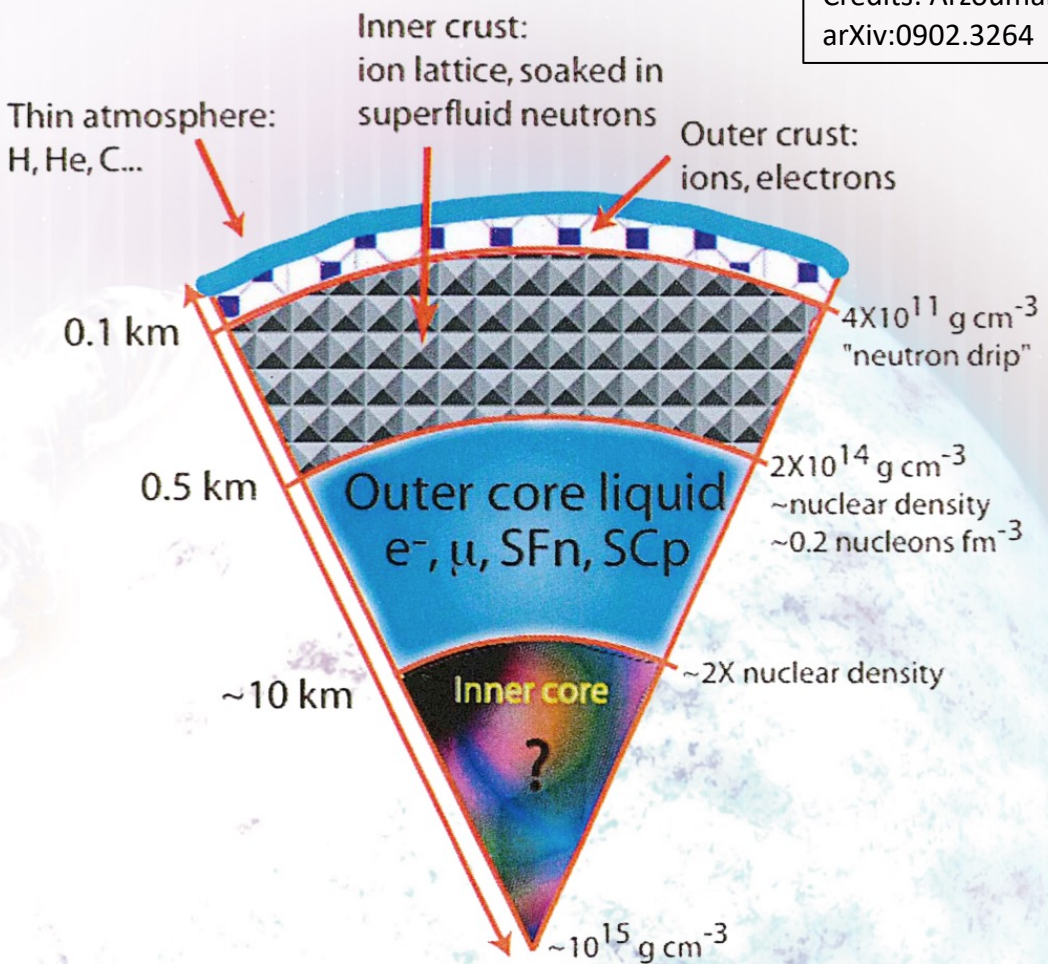

Credits: Arzoumanian et al., arXiv:0902.3264 2009.

The detection of the GW signal will allow to probe the NS internal structure providing insights into the ground state of nuclear matter in extreme conditions ~10^{15} g/cm ^{3} : nearly above above the nuclear density

All-sky Continuous-Wave searches

https://journals.aps.org/prd/abstract/10.1103/PhysRevD.100.024004

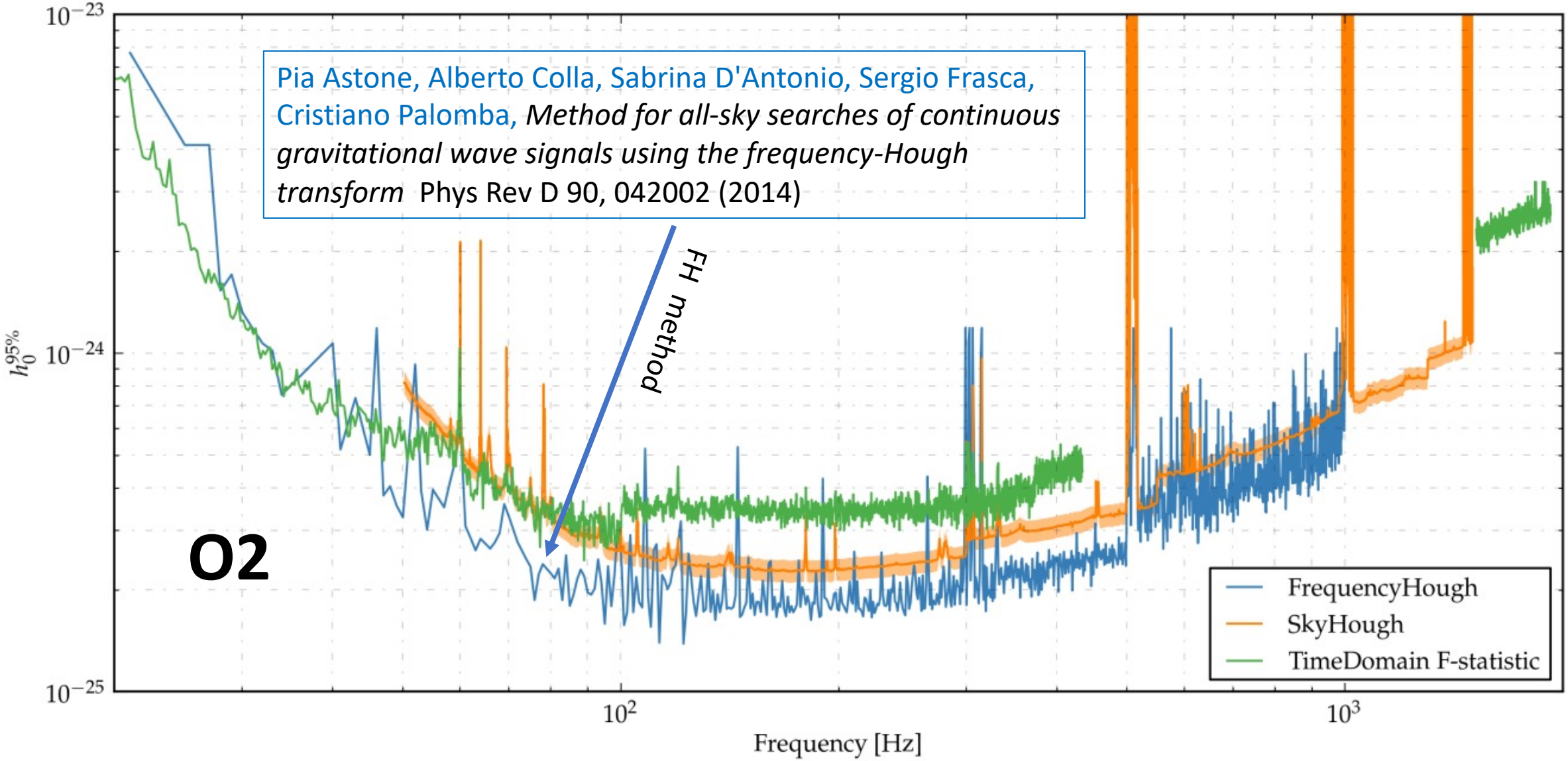

A glance to the future of GW science

O5, Post O5 Detectors toward the Einstein Telescope

More events at high SNR needed to progress on GW physics

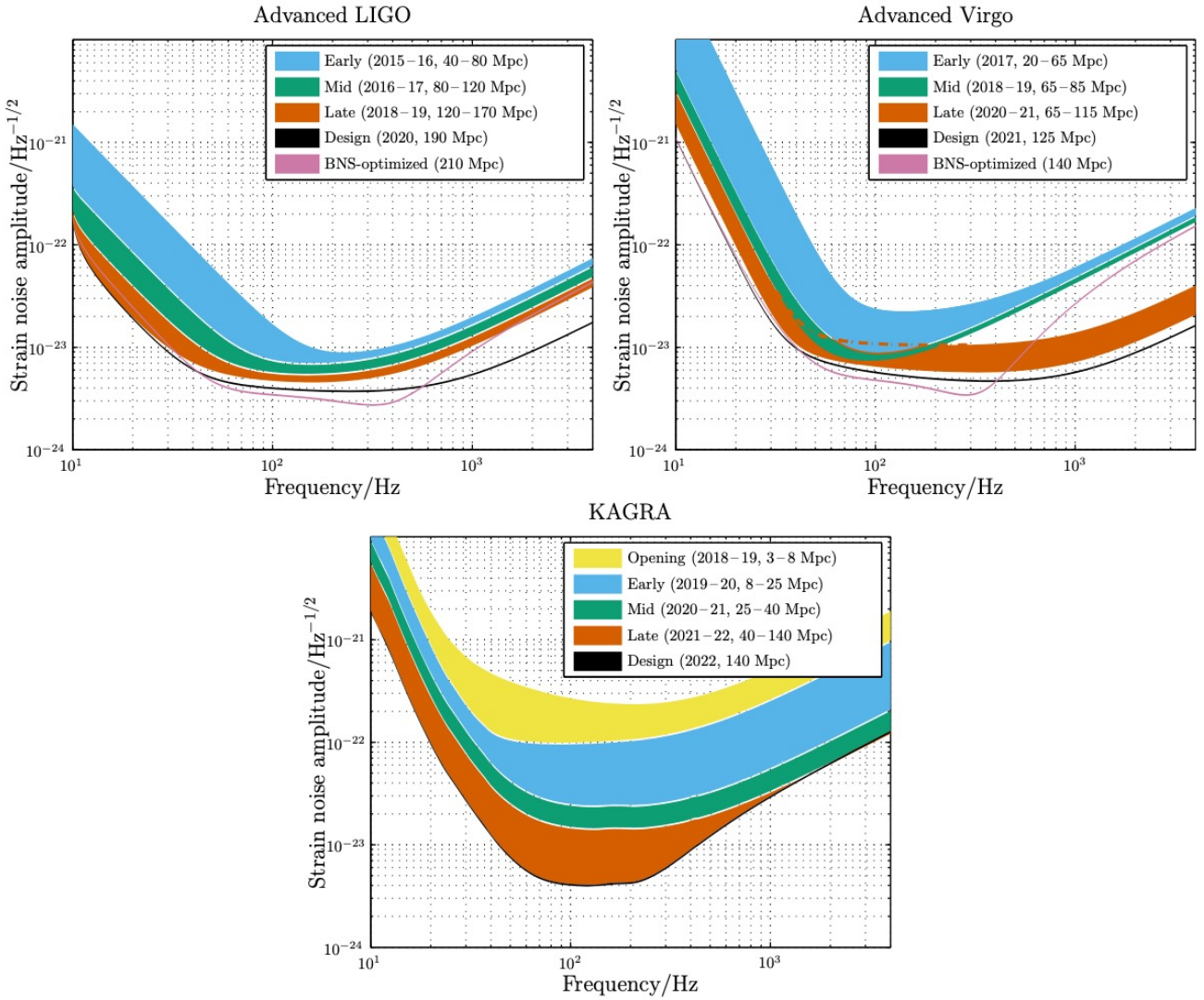

AdV + Phase II: toward O5

- Larger beams on end test masses
  - 6 cm radius ➔ 10 cm radius

- Larger end mirrors
  - 35 cm ϕ ➔ 55 cm ϕ
  - 40 kg ➔100 kg

- Better mirror coatings
  - Lower mechanical losses, less point defects, better uniformity

- New suspensions/seismic isolators for large mirrors

- Further increase of laser power

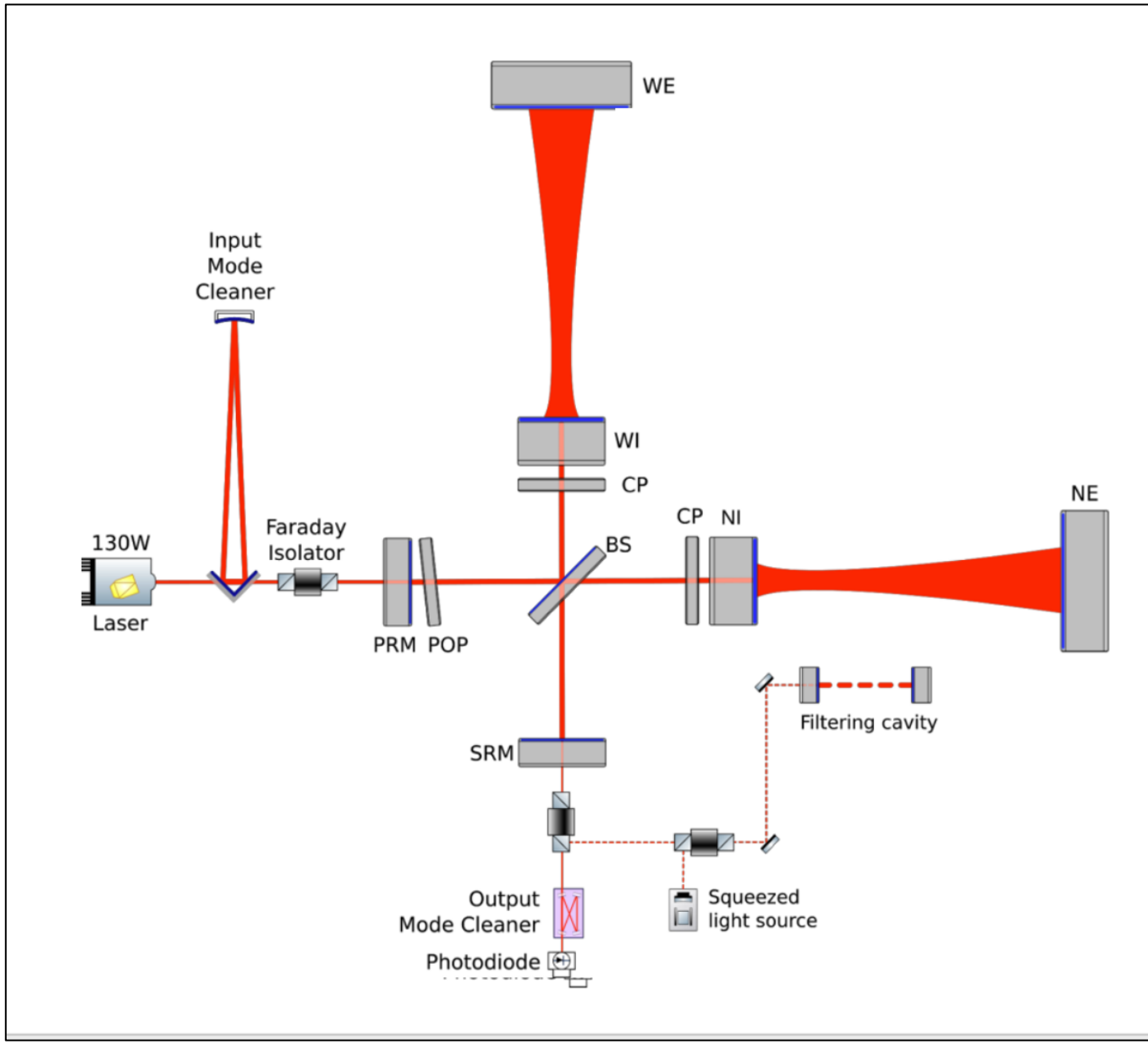

The main challenge

credits : A. Chiummo

The challenge comes from optical design:

to enlarge the beam on the test masses, arm cavities closer to instability

- Trickier controls
- Polishing requirements more strict
- More sensitive to aberrations

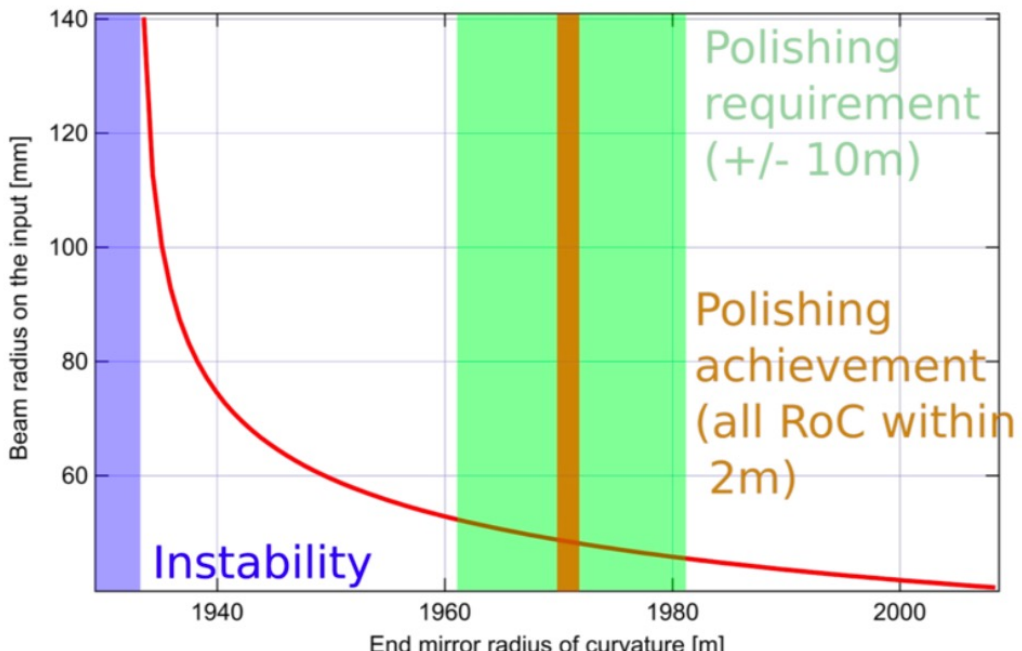

	Phase I	Phase II
End Mirror Diameter	350 mm	550 mm
Beam radious on End Mirrors	58 mm	91 mm
Beam radious on Input Mirrors	49 mm	49 mm
Radious of Curvature - End Mirror	1683 mm	1969 mm
Radious of Curvature - Input Mirror	1420 mm	1067 mm
g ➔ stability factor of the cavity	0.87	**0.95**

Larger g-factor requires:

- Tighter angular control requirements during pre-alignment ➔ 0.2 microrad
- Tight requirements RoC control ➔ ΔRoC~0.3 m

Action on Thermal Compensation System:

several upgrades foreseen for O5 on the sensing and actuation systems

Advanced Detectors in the post O5 era: the Virgo_nEXT case

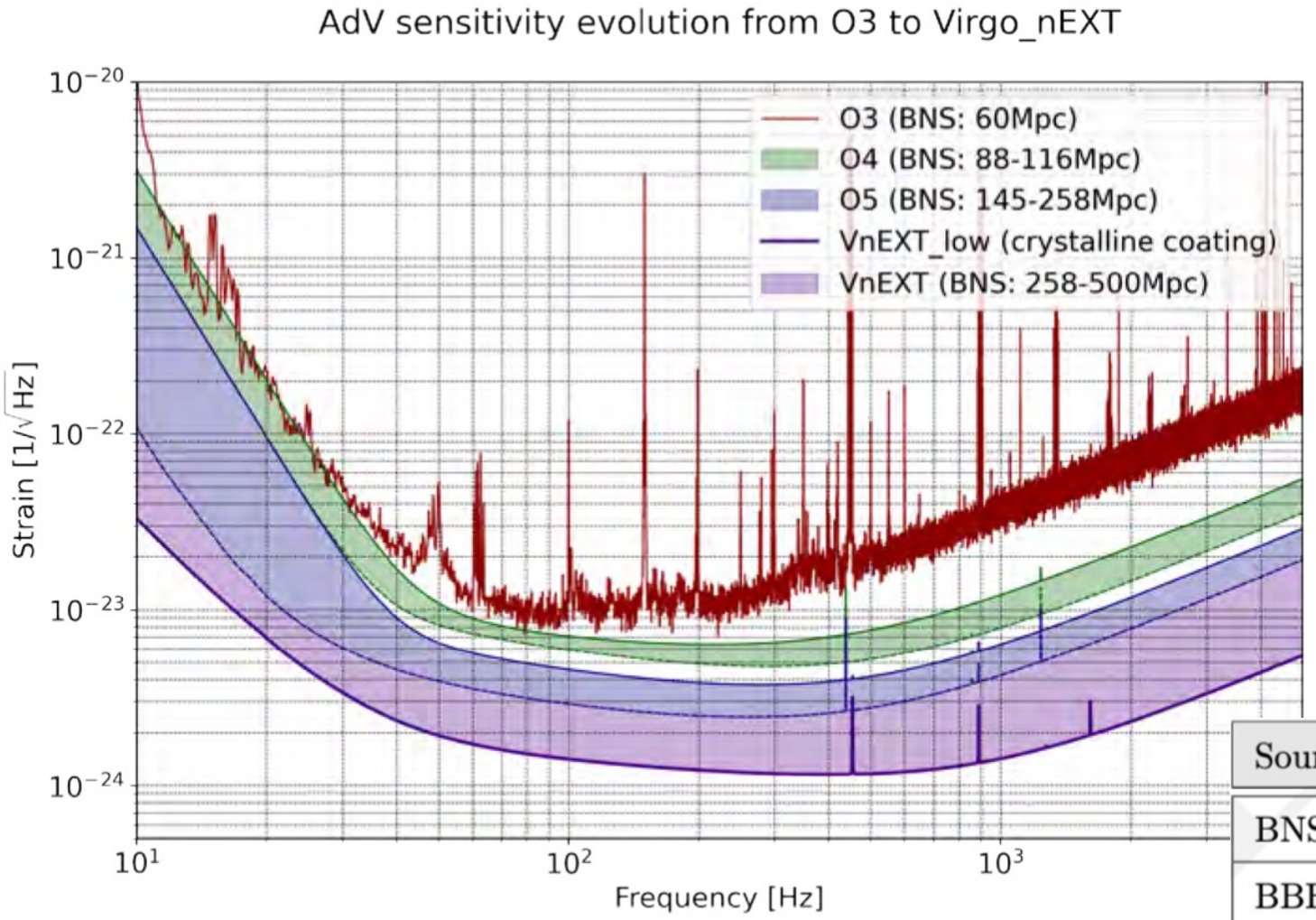

Source	O5 low	"post-O5low"
BNS range (Mpc)	258	500
BBH range $(30 + 30\,M_\odot)$ (Mpc)	590	3320
Stochastic Omega	7.5e-10	2.3e-10
Supernova (kpc) [217]	18.3	51.0

From Advanced Virgo + to Virgo_nEXT: the system upgrades

Parameter	O4 high	O4 low	O5 high	O5 low	VnEXT_low
Power injected	25 W	40 W	60 W	80 W	277 W
Arm power	120 kW	190 kW	290 kW	390 kW	1.5 MW
PR gain	34	34	35	35	39
Finesse	446	446	446	446	446
Signal recycling	Yes	Yes	Yes	Yes	Yes
Squeezing type	FIS	FDS	FDS	FDS	FDS
Squeezing detected level	3 dB	4.5 dB	4.5 dB	6 dB	10.5
Payload type	AdV	AdV	AdV	AdV	Triple pendulum
ITM mass	42 kg	42kg	42 kg	42 kg	105 kg
ETM mass	42 kg	42kg	105 kg	105 kg	105 kg
ITM beam radius	49 mm	49 mm	49 mm	49 mm	49 mm
ETM beam radius	58 mm	58 mm	91 mm	91 mm	91 mm
Coating losses ETM	2.37e-4	2.37e-4	2.37e-4	0.79e-4	6.2e-6
Coating losses ITM	1.63e-4	1.63e-4	1.63e-4	0.54e-4	6.2e-6
Newtonian noise reduction	None	1/3	1/3	1/5	1/5
Technical noise	“Late high”	“Late low”	“Late low”	None	None
BNS range	90 Mpc	115 Mpc	145 Mpc	260 Mpc	500 Mpc

Looking into the future:
2G, 2.5G and….. 3G GW detectors on the Earth

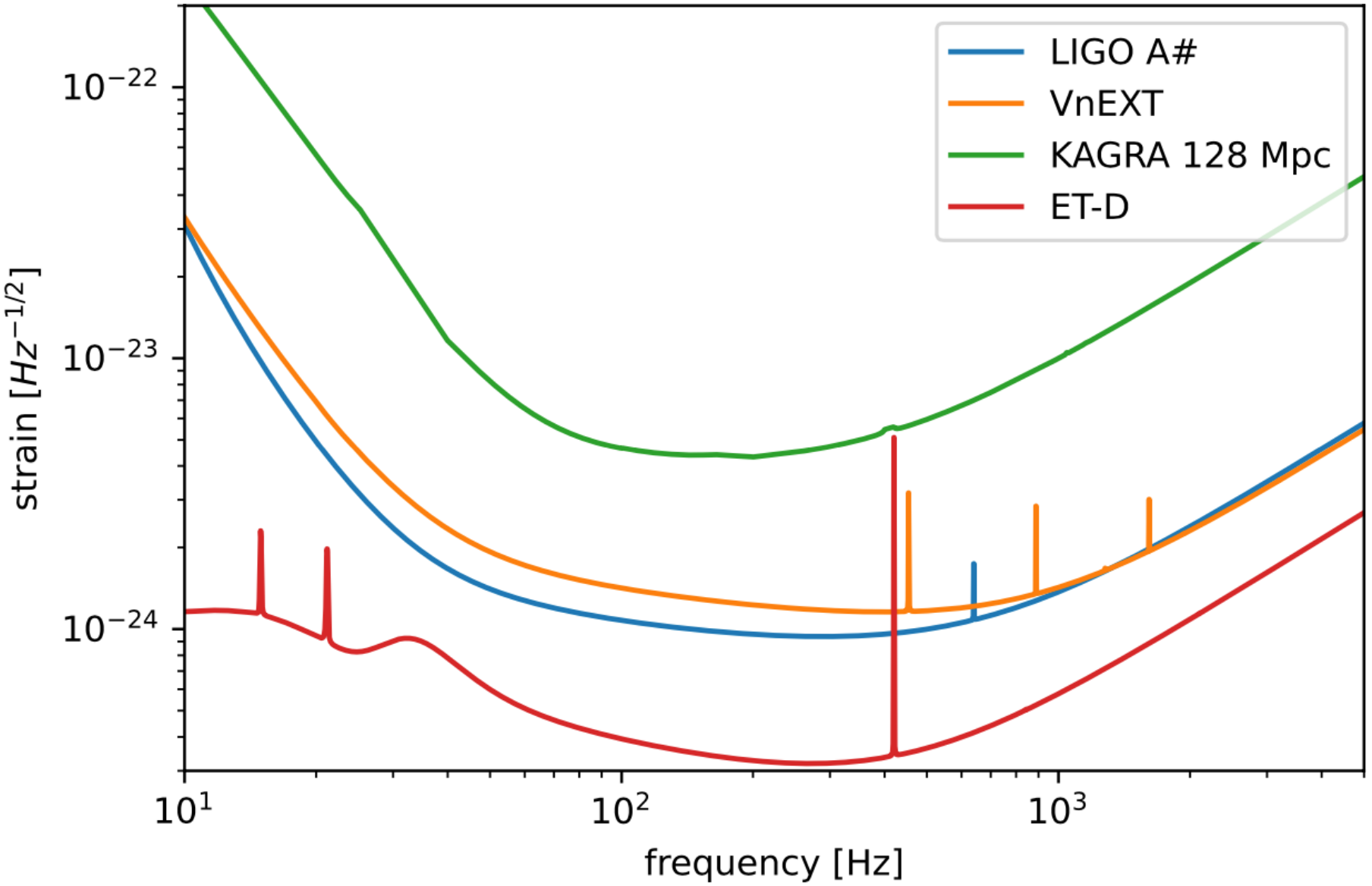

ET EINSTEIN TELESCOPE

Einstein Telescope, la sfida di Lula

Nel silenzio di Sos Enattos i 15 sismometri rilevano un sisma in Albania

Marilena Orunesu
INVIATA

LULA. Il primo sismometro, infisso nella collina che sovrasta la miniera, ha già registrato un terremoto in Albania: quarto grado. Altri strumenti, operativi sotto terra, in profondità, seguono il movimento delle correnti marine tra Francia e Corsica e perfino delle onde oceaniche a Gibilterra. Tutto pulsa nel vasto silenzio di Sos Enattos, miniera storica di Lula diventata laboratorio scientifico di prim'ordine al punto da concorrere all'Einstein Telescope, osservatorio internazionale d'avanguardia per lo studio delle onde gravitazionali

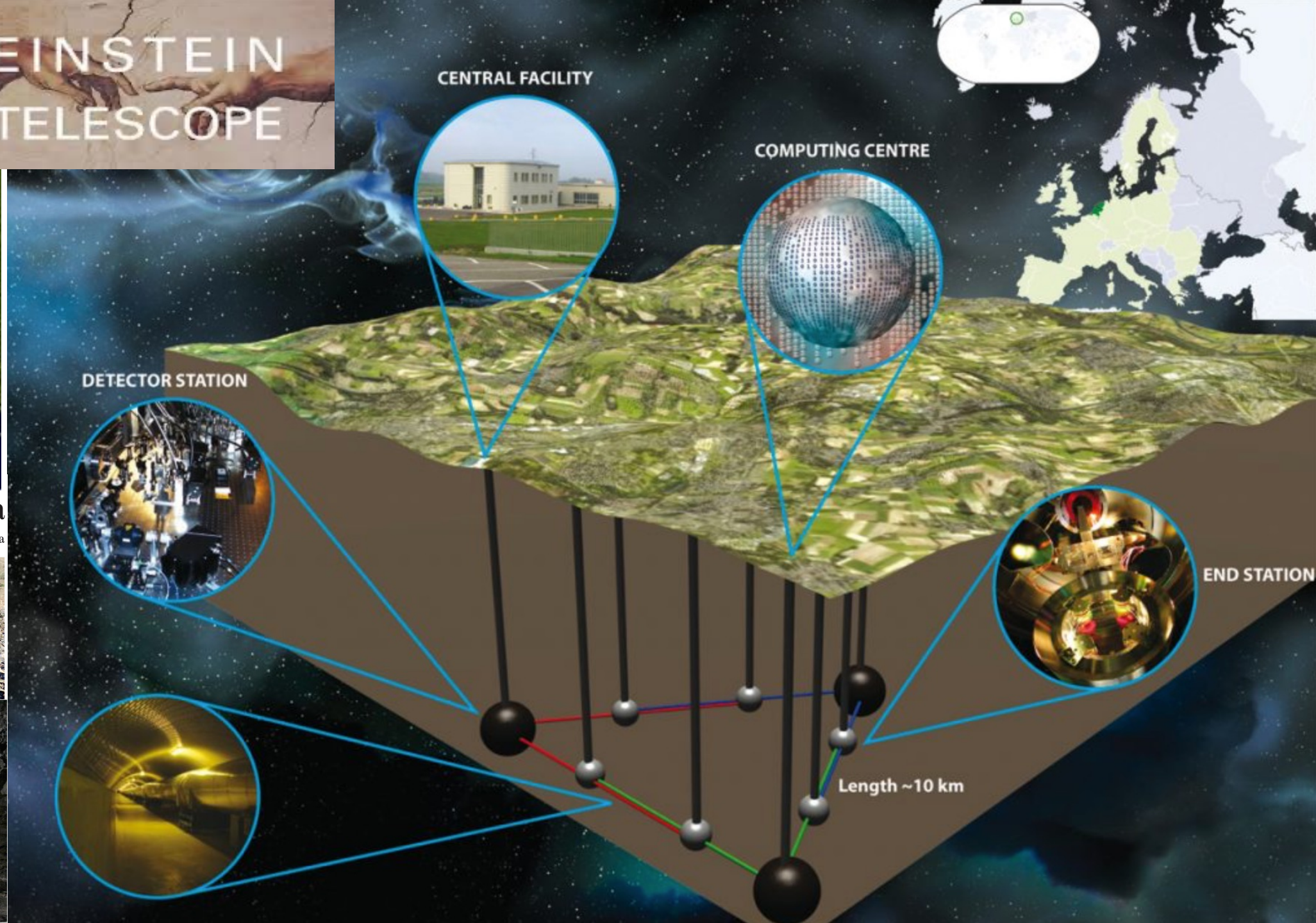

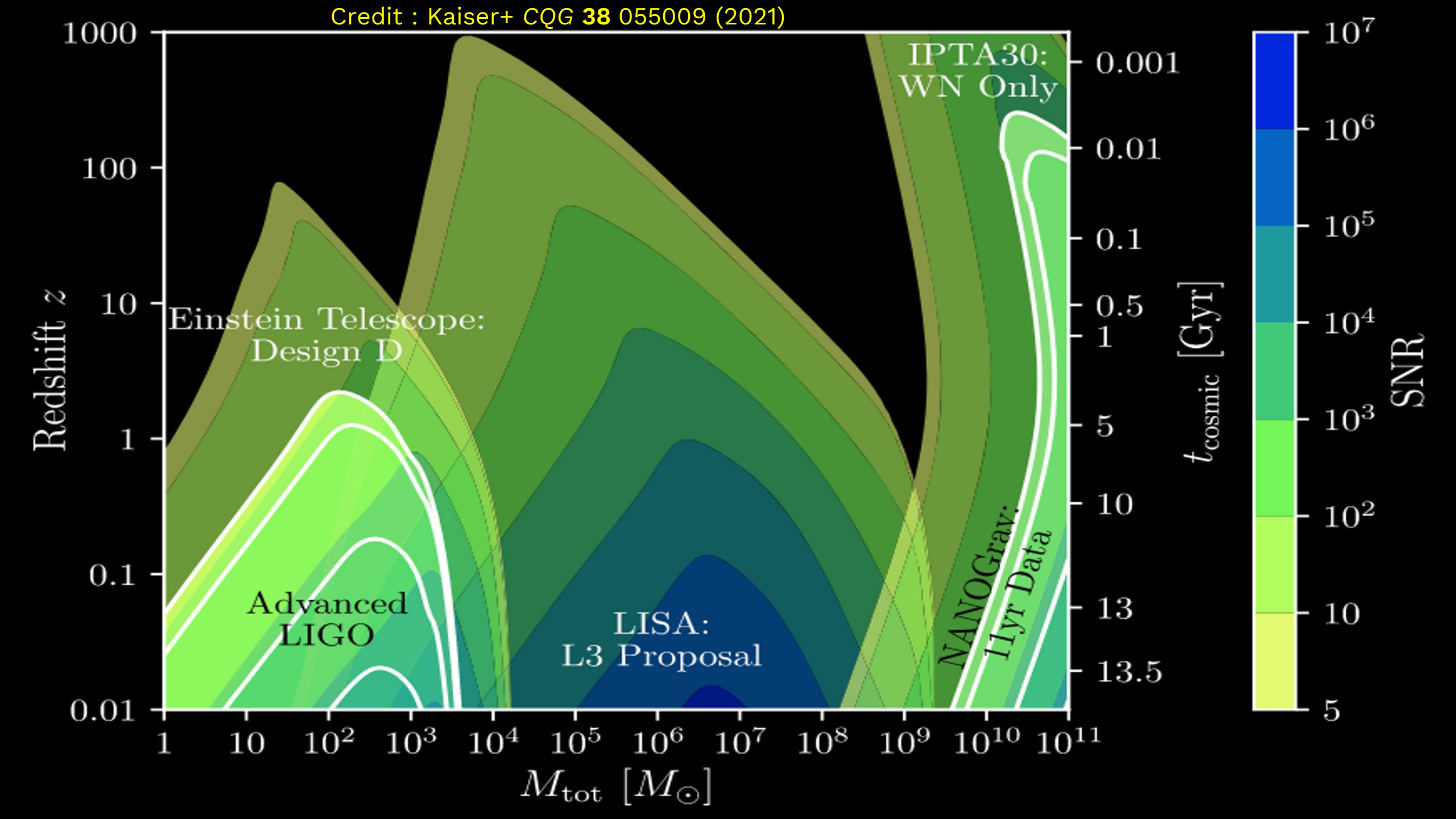
Credit : Kaiser+ CQG 38 055009 (2021)
IPTA30:
WN Only
Einstein Telescope:
Design D
Advanced
LIGO
LISA:
L3 Proposal
NANOGrav:
11yr Data
Redshift z
$M_{\rm tot}$ $[M_\odot]$
$t_{\rm cosmic}$ [Gyr]
SNR
1000
100
10
1
0.1
0.01
1
10
10^2
10^3
10^4
10^5
10^6
10^7
10^8
10^9
10^{10}
10^{11}
0.001
0.01
0.1
0.5
1
5
10
13
13.5
10^7
10^6
10^5
10^4
10^3
10^2
10
5

Detection horizon for black-hole binaries

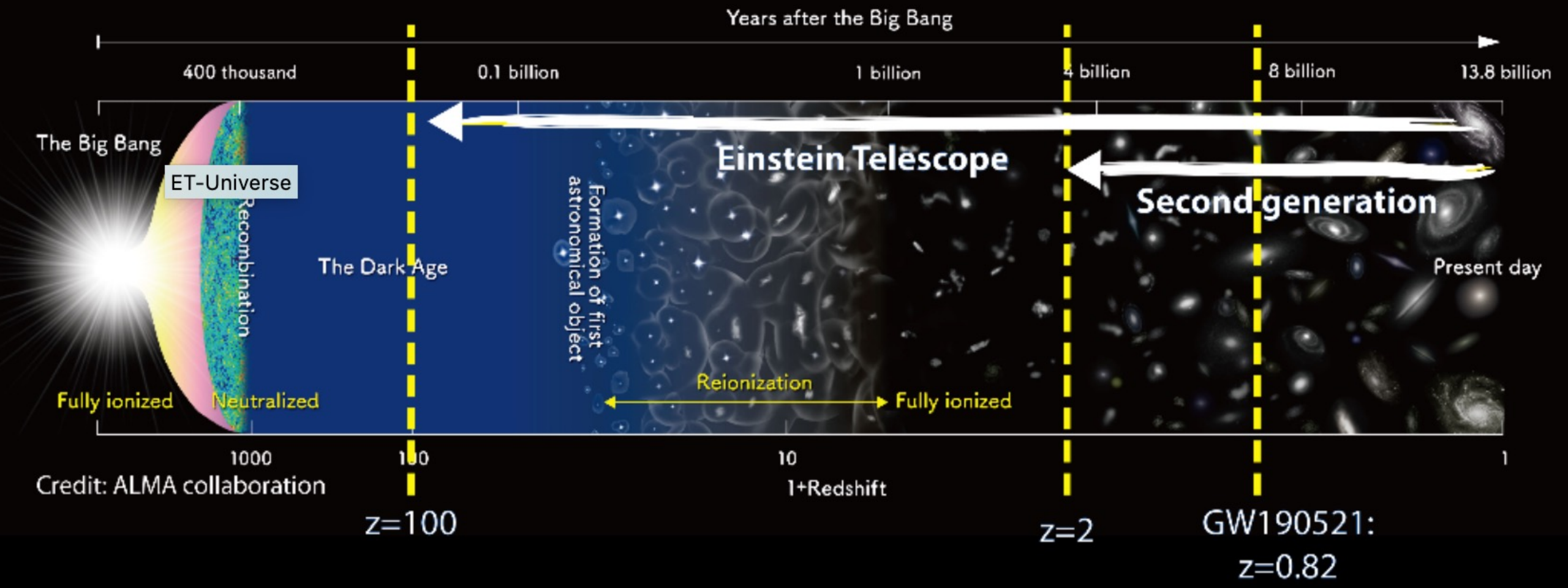

International Pulsar Timing Array

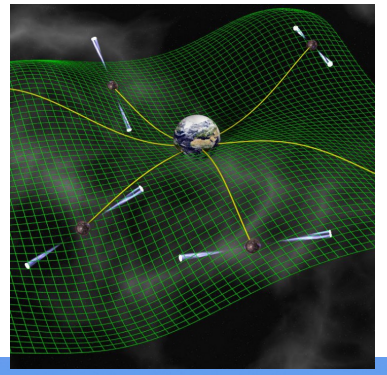

LISA:
Opens the low-frequency gravitational universe

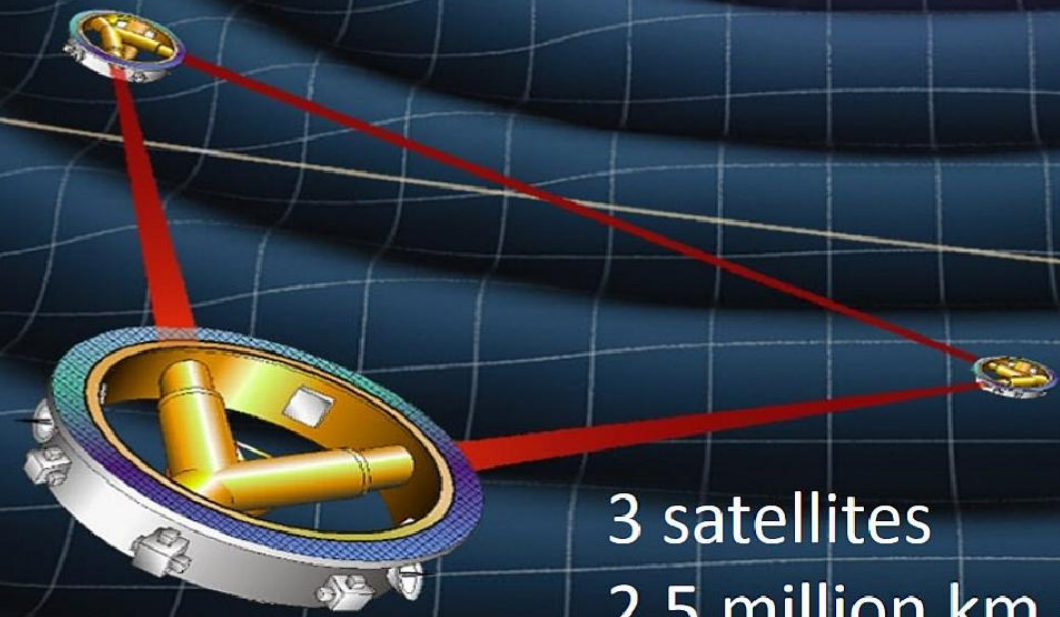

3 satellites
2.5 million km arms
50 million km behind Earth

Conclusions

The detectors of the LIGO-Virgo-KAGRA network are in the commissioning phase to improve their sensitivity and start the Science run O4 inf the spring 2023

At present 90 GW events have been collected and reported in the GW catalogue. These signals are mainly due to the BBH coalescence.

A couple of events provide hints toward new directions for the modelling the BH and BBH formation theories.

New challenges are the detection of continuous gravitationl waves from isolated rotating NS

Advanced+ detectors will play this game waiting for….. IPTA, LISA and EINSTEIN TELESCOPE to explore the entire universe with GW

EXTRA SLIDES

Mir

$$M = \begin{pmatrix} -\sqrt{R} & \sqrt{T} \\ \sqrt{T} & \sqrt{R} \end{pmatrix}$$

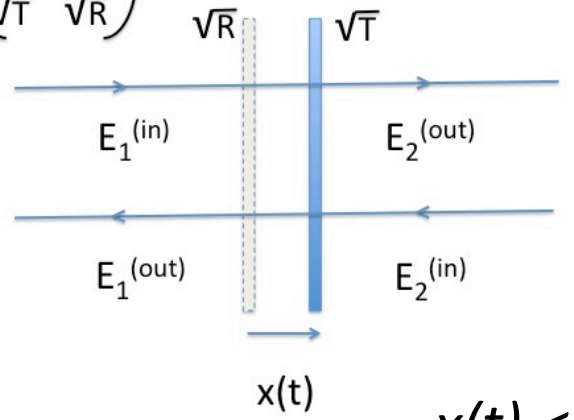

$$E_1^{(out)}(t) = -\sqrt{R}E_1^{(in)}\left(t - 2x(t)/c\right) + \sqrt{T}E_2^{(in)}(t)$$

$$E_2^{(out)}(t) = \sqrt{T}E_1^{(in)}(t) + \sqrt{R}E_2^{(in)}\left(t + 2x(t)/c\right)$$

$$x(t) << \omega/(2\pi c)$$

The output electric fields are phase modulated by the mirror motion

The modulation effect is encoded just in the s-quadrature of the electric field.

The light spectral component $L_s(\Omega)$ containing information of the motion x (with spectral component $X(\Omega)$) is proportional to the incoming light $\mathcal{E}_0$

$$L_s(\Omega) = (\omega_0/2\pi c)\ X(\Omega)\ \mathcal{E}_0$$

Quantum Interferometer with squeezed e.m. vacuum

- Electromagnetic fields are quantized:

$$\hat{E} = \hat{X}_1 \cos\omega t + i\hat{X}_2 \sin\omega t$$

- Quantum fluctuations exist in the vacuum state:

$$\langle(\Delta\hat{X}_1)^2\rangle \langle(\Delta\hat{X}_2)^2\rangle \geq 1$$

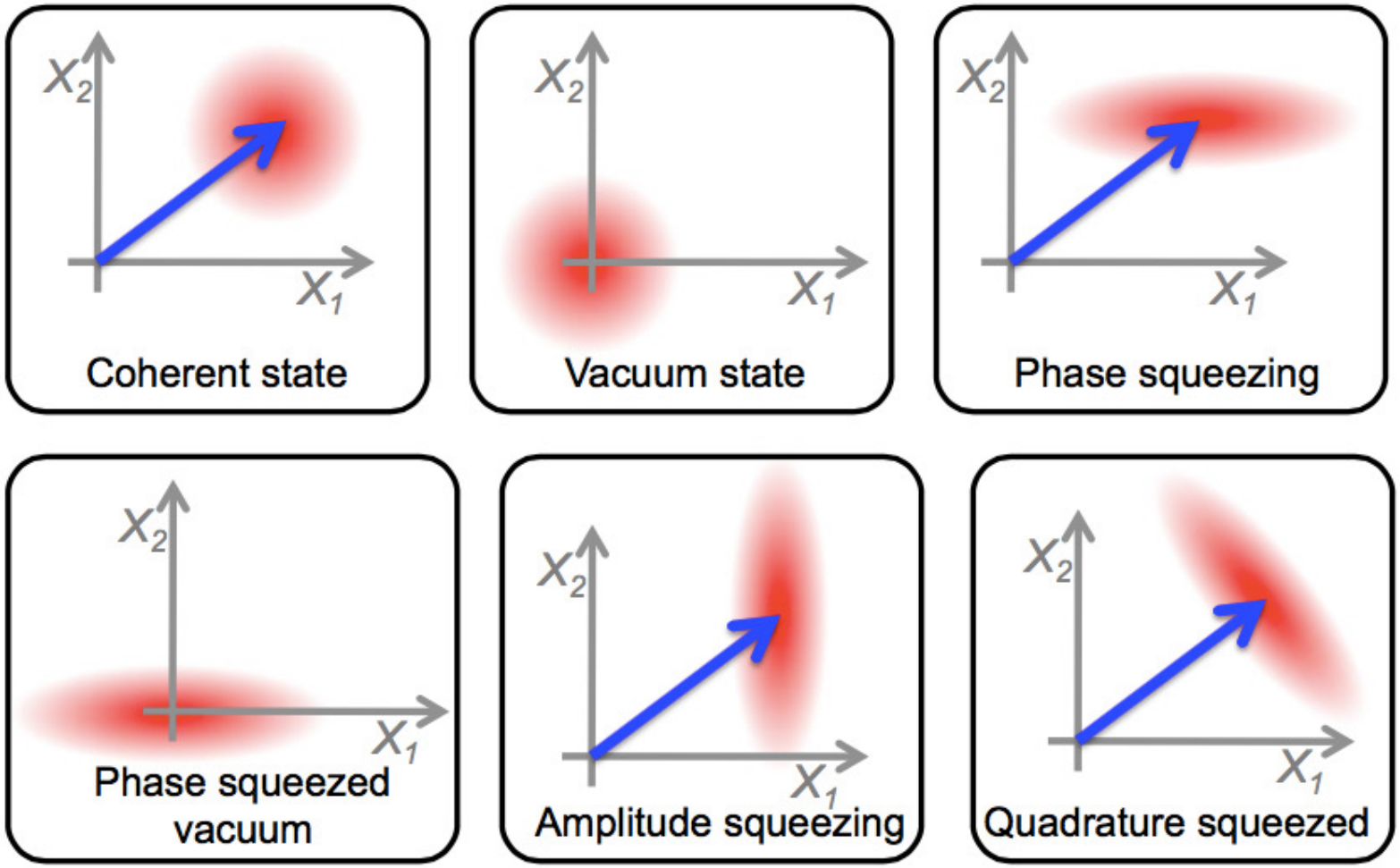

Frequency-Hough: robustness for CW signal clusters

[PRD, **106**, 042009 (2022)]

1. In general, if signals form dense clusters, the spectral autoregressive estimator (red) could be affected

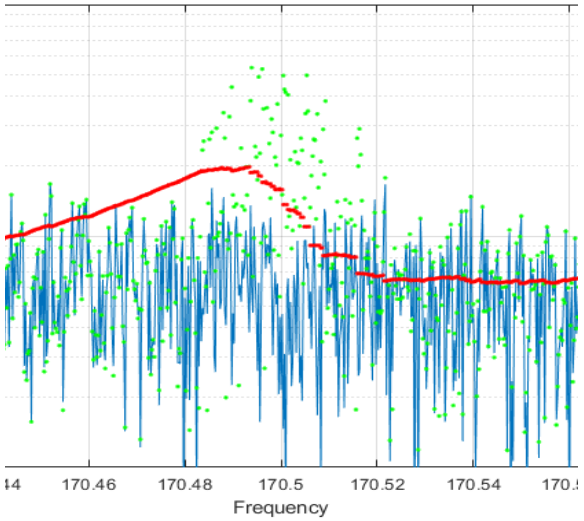

2. The annual and daily Doppler effects are a powerful signature to resolve signals from different sources

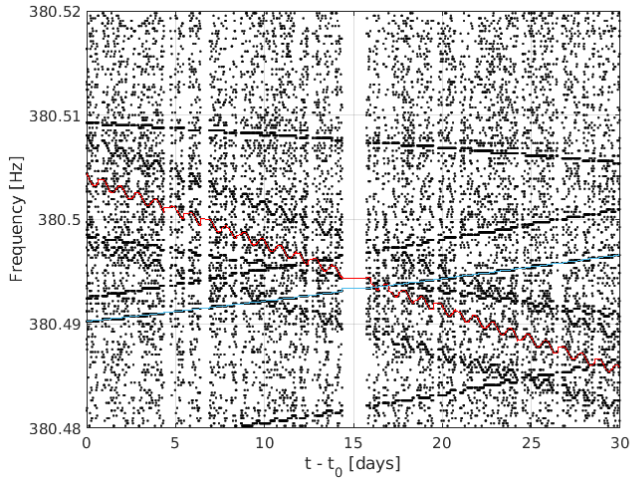

3. ***Crucial index***: cluster frequency width VS spectral estimator memory

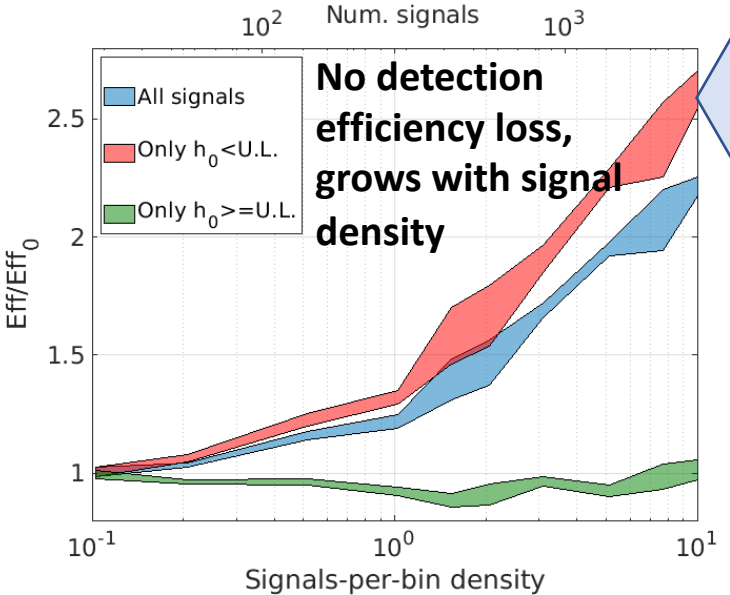

Frequency width ≲ estimator memory

The estimator is not fast enough to adapt to the signal mountain, which remains well above the noise floor

The estimator is able to adapt to the varied noise floor; signals can fall under the selection threshold
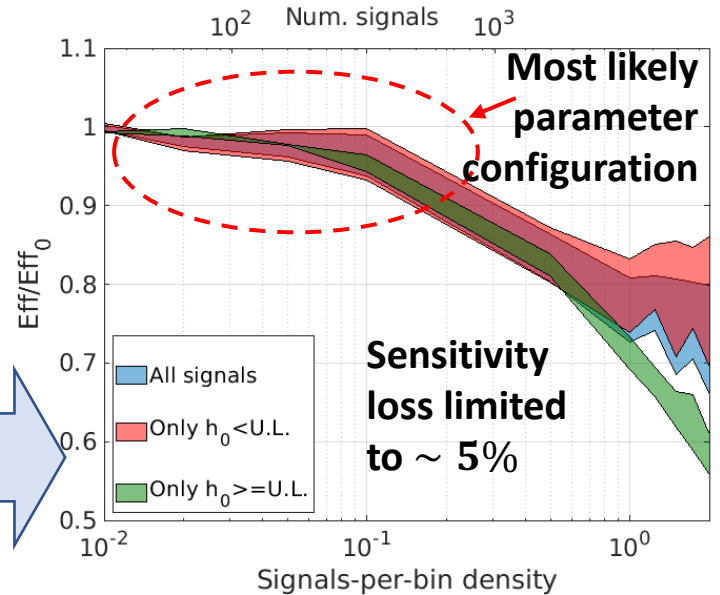
Frequency width ≫ estimator memory